LBL-24875 c.2
UC-406

Lawrence Berkeley Laboratory
UNIVERSITY OF CALIFORNIA

Engineering Division

Generation of the J_c, H_c, T_c Surface for Commercial Superconductor Using Reduced-State Parameters

M.A. Green

April 1988

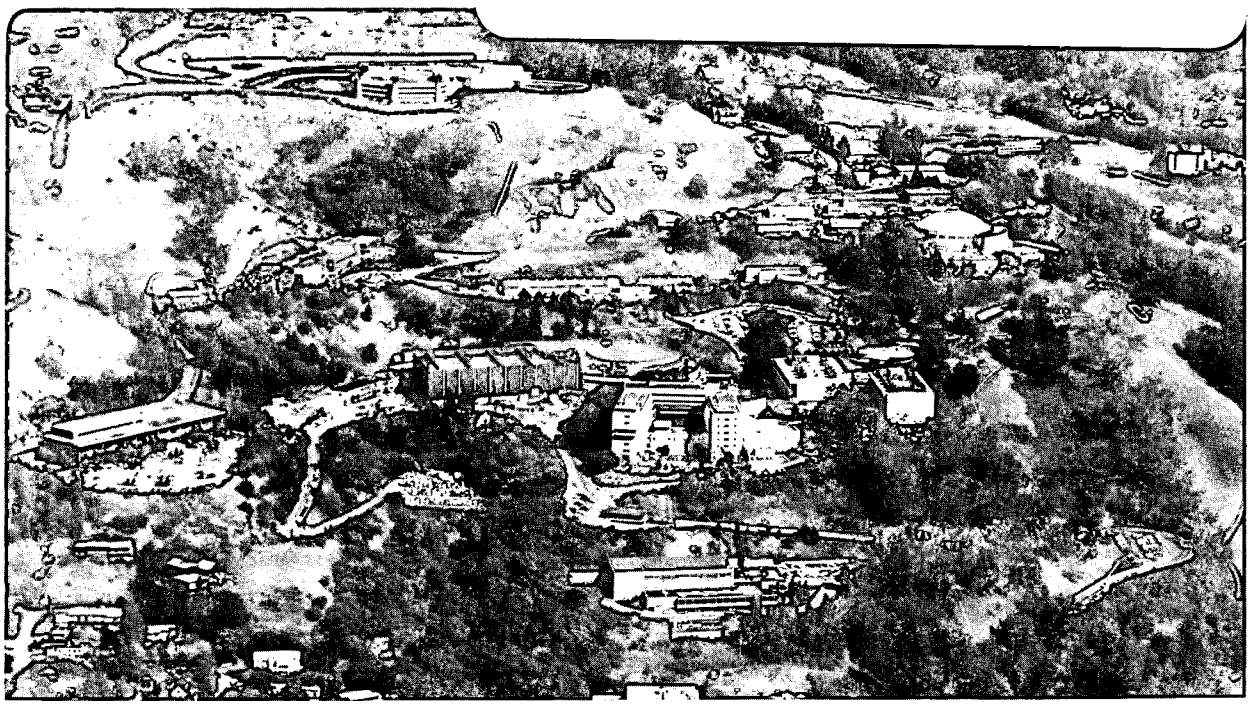

Prepared for the U.S. Department of Energy under Contract Number DE-AC03-76SF00098.

DISCLAIMER

SSC-N-502
LBL-24875

GENERATION OF THE J_c, H_c, T_c SURFACE FOR COMMERCIAL SUPERCONDUCTOR USING REDUCED-STATE PARAMETERS

Michael A. Green

Lawrence Berkeley Laboratory
University of California
Berkeley, CA 94720

April 1988

This work was supported by the U. S. Department of Energy under Contract No. DE-AC03-76SF00098.

Generation of the J_c, H_c, T_c Surface for Commercial Superconductor Using Reduced-State Parameters

Michael A. Green
Lawrence Berkeley Laboratory
1 Cyclotron Road
Berkeley, CA 94720

April 1988

ABSTRACT

This report presents a method for calculating the J_c, H_c, T_c surface for Type II superconductors. The method requires that one knows T_c at zero current and field, H_{c2} at zero current and temperature, and J_c at at least one temperature and field. The theory presented in this report agrees with measured data quite well over virtually the entire J_c, H_c, T_c surface given the value of J_c versus H at one or two temperatures. This report presents calculated and measured values of J_c versus T and B for niobium titanium, niobium zirconium, niobium tin, niobium titanium tin, niobium tantalum tin, vanadium zirconium hafnium, and vanadium gallium. Good agreement of theory with measured data was obtained for commercial niobium titanium and niobium tin.

TABLE OF CONTENTS

BACKGROUND

There is often the need to know the behavior of a commercial Type II superconductor under conditions different from those measured by the manufacturer. For example, one often knows the superconductor critical current (critical current density, J_c) as a function of magnetic field (or magnetic induction, B) at the boiling point of helium (T = 4.22 K) over a limited range of magnetic inductions (e.g., 2 T to 8 T). Suppose, however, one wants to know the critical current density over a wide range of magnetic inductions (from 0 to B_{c2}) at a temperature of, e.g., 3.0 K. The measured data are often unavailable and costly to obtain. This report presents a method by which one can calculate the critical surface for a commercial superconductor given only the upper critical field, H_{c2}, the critical temperature, T_c, and some values of the critical current versus magnetic field at the boiling point of helium (or any other temperature).

The reduced critical state method is similar to the methods used to calculate the thermodynamic properties of a fluid. The J_c, B, T surface represents the phase change surface for a superconductor. The reduced critical state method presented here uses reduced critical temperature, reduced critical induction and reduced critical current density to calculate the entire J_c, T, B surface for superconductors such as niobium titanium.

The value of this method is demonstrated when one needs to calculate the effects of superconductor magnetization on the field in a dipole magnet (such as the SSC dipole) over various accelerator operating temperatures. The reduced state method was used to calculate the three dimensional J_c, B, T surface for niobium titanium shown in Figure 24 on page 60.

THE REDUCED-CRITICAL-STATE METHOD

The method used to calculate the critical surface for a commercial Type II superconductor is based on the following assumptions:

1) The critical temperature, T_c, at zero field and the upper critical field, H_{c2}, at zero temperature are functions only of the alloy or chemical composition of the superconductor.
2) The critical current density, J_c, is a function of the metallurgical treatment of the superconductor such as heat treatment and cold work, where as T_c and H_{c2} are independent of the treatment of the superconductor. (In most commercial materials this assumption is reasonably valid.)
3) The critical current of the superconductor varies linearly with temperature. (For commercial material, this is true above 3.5 K.)
4) J_c-versus-B is given at one temperature over a range of magnetic fields.
5) In the absence of a complete J_c-versus-B curve (particularly at low fields), the ratio of $J_c(T,B)/J_c(T,5\ T)$ is identical for all materials of the same alloy or chemical composition.

The assumptions given above are reasonably valid for commercial niobium titanium[1-5] and commercial niobium tin.[3,6,7]

If the above assumptions given are correct, one should be able to estimate J_c anywhere on the superconductor critical surface if one knows: (1) J_c versus magnetic induction, B, at a given temperature less than the T_c at zero field and (2) T_c versus B at zero J_c. A reduced-critical state-model says that T_c as a function of magnetic field (or induction) at zero current

can be determined provided one knows the zero-field value of critical temperature, $T_c(0)$, and the zero-temperature value of the upper critical field $H_{c2}(0)$ [or upper critical induction $B_{c2}(0)$].

Reduced Critical Temperature Versus Reduced Critical Field

The reduced critical temperature, T_{cR}, and the reduced critical field, H_{cR}, are defined as follows:

$$T_{cR} = \frac{T_c(B)}{T_c(0)} , \tag{1}$$

when J_c is zero, and

$$H_{cR} = \frac{H_{c2}(T)}{H_{c2}(0)} , \tag{2}$$

when J_c is zero. One can define upper critical induction (tesla) given upper critical field (A m^{-1}) using the following relationship:

$$B_{c2} = \mu_o H_{c2}, \tag{3}$$

where μ_o is the permeability of air ($4\pi \times 10^{-7}$ H m^{-1}). Thus, the reduced critical induction, B_{cR}, can be defined as follows:

$$B_{cR} = \frac{B_{c2}(T)}{B_{c2}(0)} = \frac{H_{c2}(T)}{H_{c2}(0)} = H_cR . \tag{4}$$

From Lubell,[8] B_{cR} can be stated in terms of temperature T_{cR} using the following relationship:

$$B_{cR} = 1 - (T_{cR})^N, \tag{5}$$

where N is some number less than two. Lubell states that N = 1.7 fits measured data for niobium titanium over a reasonable temperature range. The fit, according to Lubell, is not very good below 3 K; thus he suggests that a more complicated equation can be used. A look at niobium-titanium reduced-temperature data[1,5,8] suggests that N = 1.67 will give a somewhat better fit but that an even-better fit can be achieved using a mixed quadratic and linear equation. A fit of niobium-titanium data suggests the following reduced forms:

$$B_{cR} = 1 - 1.1762\ (T_{cR})^2 \tag{6a}$$

for $T_{cR} \leq 0.613$, and

$$B_{cR} = 1.442 - 1.442\ T_{cR} \tag{6b}$$

for $T_{cR} \geq 0.613$.

Figure 1 shows that Eqs. (6a) and (6b) fit to a measured value of B_{cR} versus T_{cR} for niobium titanium. Also included in Fig. 1 are commercial samples of niobium titanium tantalum, niobium zirconium, niobium-tin ribbon, and multifilamentary niobium tin in a bronze matrix. Tables 1[1-7,9-11] and 2 present the material parameters for the materials in Fig. 1. All of these materials fit Eqs. (6a) and (6b) quite well.

REDUCED UPPER CRITICAL FIELD VERSUS REDUCED CRITICAL TEMPERATURE FOR VARIOUS COMMERCIAL SUPERCONDUCTORS

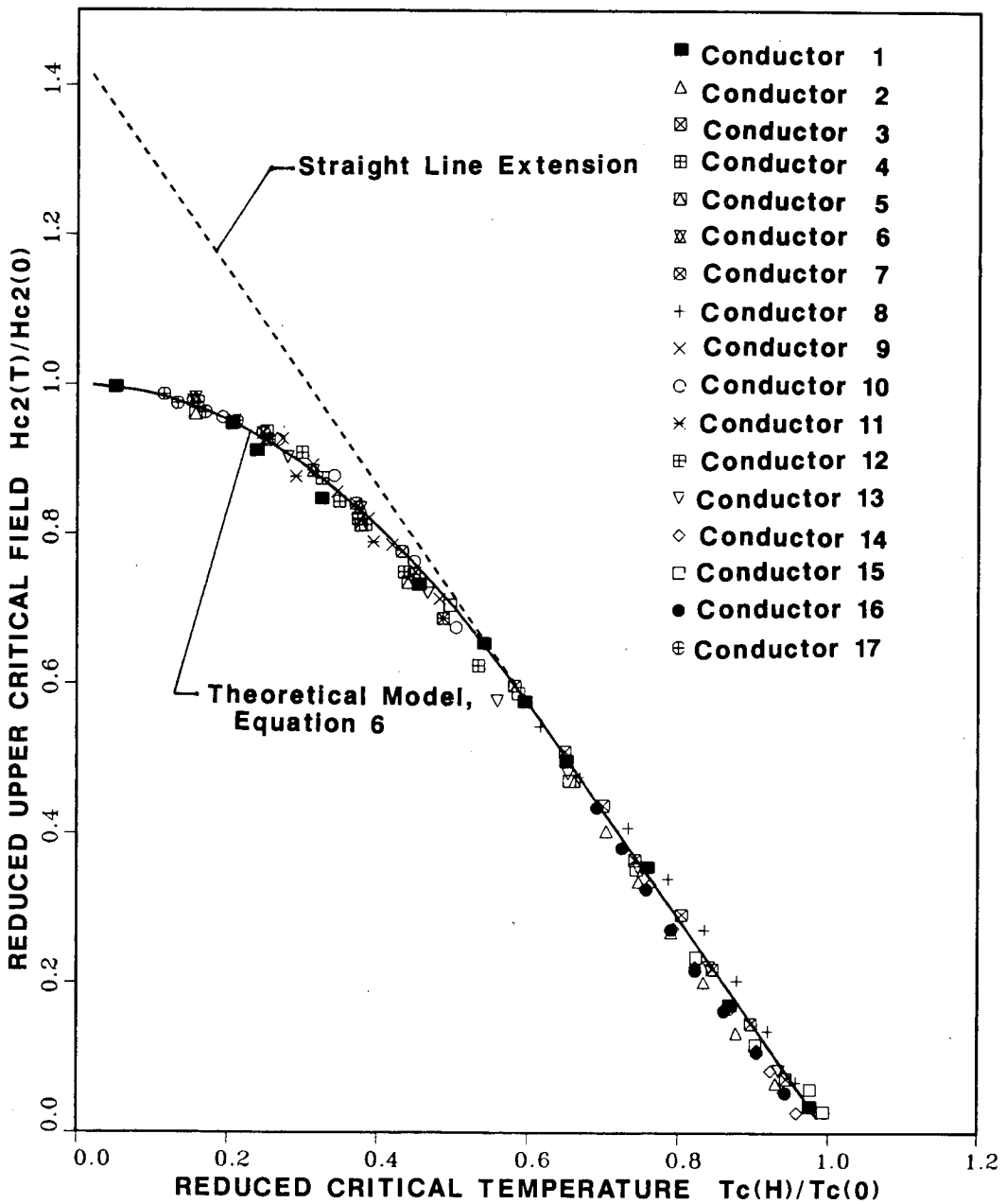

XBL 882-666

Figure 1 Reduced critical field versus reduced critical temperature for Nb-Ti, Nb-Zr, Nb-Ti-Ta and Nb_3Sn (see Tables 1 and 2)

Table 1. Commercial Superconductors Used in Figure 1
(Reduced Field Vs. Reduced Temperature)

CONDUCTOR NUMBER	DESCRIPTION OF SUPERCONDUCTOR	FORM OF SUPERCONDUCTOR	MATRIX MATERIAL	REFERENCE NUMBER	YEAR
1	Niobium-44.0 w% Titanium	Multifilament	Copper	1,2	1969-1972
2	Niobium-46.5 w% Titanium	Multifilament	Copper	3	1979
3	Niobium-53.0 w% Titanium	Multifilament	Copper	3	1979
4	Niobium-46.5 w% Titanium	Multifilament	Copper	4	1979
5	Niobium-49.7 w% Titanium	Multifilament	Copper	4	1979
6	Niobium-50.4 w% Titanium	Multifilament	Copper	4	1979
7	Niobium-52.7 w% Titanium	Multifilament	Copper	4	1979
8	Niobium-46.5 w% Titanium	Multifilament	Copper	5	1981
9	Niobium-50.0 w% Titanium	Multifilament	Copper	9	1979
10	Niobium-46.5 w% Titanium	Multifilament	Copper	10	1981
11	Niobium-43.0 w% Titanium-25 w% Ta	Multifilament	Copper	10	1981
12	Niobium-43.0 w% Titanium-25 w% Ta	Multifilament	Copper	9	1979
13	Niobium-25.0 w% Zirconium	Single Filament	Copper	6	1967
14	Niobium 3.0-Tin (A-15)	Ribbon	NA	6	1967
15	Niobium 3.0-Tin (A-15)	Multifilament	Bronze	7	1980
16	Niobium 3.0-Tin (A-15)	Multifilament	Bronze	3	1979
17	Niobium 3.0-Tin (A-15)	Multifilament	Bronze	11	1981

Table 2. The Critical Temperature at Zero Field and the Upper Critical Induction at Zero Temperature for the Commercial Superconductors in Figure 1

CONDUCTOR NUMBER	DESCRIPTION OF SUPERCONDUCTOR	Tc(0) (K)	Bc2(0) (T)
1	Niobium-44.0 w% Titanium	9.22	14.03
2	Niobium-46.5 w% Titanium	9.35	14.84
3	Niobium-53.0 w% Titanium	9.69	13.70
4	Niobium-46.5 w% Titanium	9.35	14.85
5	Niobium-49.7 w% Titanium	9.52	14.40
6	Niobium-50.4 w% Titanium	9.54	14.35
7	Niobium-52.7 w% Titanium	9.69	13.90
8	Niobium-46.5 w% Titanium	9.40	14.70
9	Niobium-50.0 w% Titanium	9.53	14.00
10	Niobium-46.5 w% Titanium	9.35	14.80
11	Niobium-43.0 w% Titanium-25.0 w% Tantalum	8.60	16.80
12	Niobium-43.0 w% Titanium-25.0 w% Tantalum	8.60	16.00
13	Niobium-25.0 w% Zirconium	10.70	8.30
14	Niobium 3.0-Tin (A-15)	17.00	18.00
15	Niobium 3.0-Tin (A-15)	16.50	17.00
16	Niobium 3.0-Tin (A-15)	16.80	17.00
17	Niobium 3.0-Tin (A-15)	16.50	16.20

Since a variety of commercial Nb-Ti, Nb-Zr and Nb_3Sn materials fit Eqs. (6a) and (6b), and Eq. (5) when N = 1.67, a number of other superconductors were investigated. Figure 2 shows B_{cR} versus T_{cR} for a variety of A-15 materials, Chevrel compounds, Laves-phase materials, and a few high-T_c superconductors. Tables 3[2-20] and 4 present the material parameters for the materials in Fig. 2.

Figure 2 shows that some materials fit the curve and others do not fit the commercial superconductor curve. If one uses the general form suggested by Lubell [see Eq. (5)], one can apply N = 1.2 to materials such as $(Nb-Ta)_3Sn$, and one can use N = 2.2 for material such as V_3Ga and $(V-Ta)_3Ga$. Most of the other materials come quite close to the N = 1.7 line.

Selection of $T_c(0)$ and $B_{c2}(0)$

Superconducting alloys such as Nb-Ti, Nb-Ti-Ta, and Nb-Zr generally have set values of $T_c(0)$. The upper critical induction $B_{c2}(0)$ quoted in the literature, often the value of surface-current critical induction $B_{c3}(0)$, is generally a little high. The value of B_{c2} where the bulk current density goes to zero can be from 0.5 to 1.2 T lower than the highest value of B_{c3}.[21,22] The critical temperature $T_c(0)$ is often a set value when the filament diameter is above 1 μm. With niobium titanium, the critical temperature is depressed as the filament diameter drops below 0.2 μm. (At 0.02-μm diameter, the value of T_c is reduced 2.4 K.[23]) The value of B_{c2} is also reduced as the filament diameter is reduced below 0.2 μm. (The value of B_{c2} in the direction perpendicular to the filament is reduced more than the value of B_{c2} in the direction parallel to the filament.)

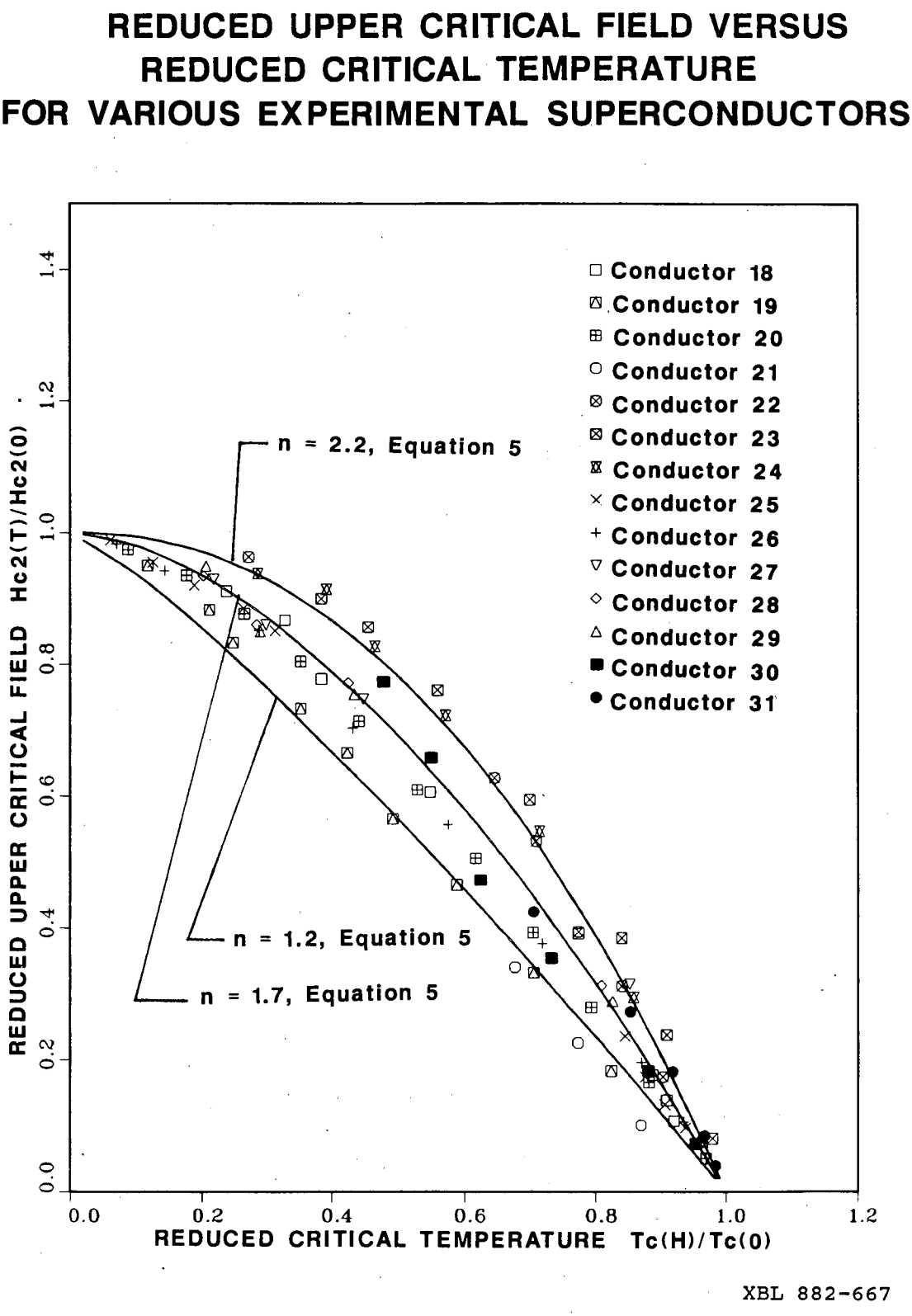

Figure 2 Reduced critical field versus reduced critical temperature for various experimental superconductors (see Tables 3 and 4)

Table 3. Experimental Superconductors Used in Figure 2
(Reduced Field Vs. Reduced Temperature)

CONDUCTOR NUMBER	DESCRIPTION OF SUPERCONDUCTOR	FORM OF SUPERCONDUCTOR	MATRIX MATERIAL	REFERENCE NUMBER	YEAR
18	Niobium 3-Silicon (A-15)	Flakes	NA	12	1979
19	(Niobium-Tantalum) 3-Tin (A-15)	Multifilament	Bronze	13	1985
20	Niobium 3-Germanium (A-15)	---	NA	14	1983
21	Niobium 3-Germanium (A-15)	Thin Film	NA	15	1981
22	Vanadium 3-Gallium (A-15)	Multifilament	Bronze	16	1985
23	Vanadium 3-Gallium (A-15)	Thin Film	NA	17	1985
24	Vanadium 0.735-Tantalum 0.015-Gallium 0.25	Thin Film	NA	17	1985
25	Niobium Nitride (B-1)	Thin Film	NA	18	1983
26	$Gd_{0.2}$-Pb-Mo_6-S_8 (Chevrel Phase)	---	NA	14	1983
27	V_2 (Hf, Zr) 35 a% Zr (Laves Phase C-15)	Multifilament	V-Hf	19	1985
28	V_2 (Hf, Zr) 45 a% Zr (Laves Phase C-15)	Multifilament	V-Hf	19	1985
29	V_2 (Hf, Zr) 50 a% Zr (Laves Phase C-15)	Multifilament	V-Hf	19	1985
30	$La_{1.85}$ $Sr_{0.15}$ Cu O_{4-Y} (High Tc)	Block	NA	20	1987
31	$Y_{0.4}$ $Ba_{0.6}$ Cu $O_{2.22}$ (High Tc)	Block	NA	20	1987

Table 4. The Critical Temperature at Zero Field and the Upper Critical Induction at Zero Temperature for the Experimental Superconductors in Figure 2

CONDUCTOR NUMBER	DESCRIPTION OF SUPERCONDUCTOR	Tc(0) (K)	Bc2(0) (T)
18	Niobium 3-Silicon (A-15)	17.7	15.8
19	(Niobium-Tantalum) 3-Tin (A-15)	17.0	30.0
20	Niobium 3-Germanium (A-15)	22.7	38.5
21	Niobium 3-Germanium (A-15)	20.7	35.8
22	Vanadium 3-Gallium (A-15)	15.5	21.8
23	Vanadium 3-Gallium (A-15)	14.3	21.0
24	Vanadium 0.735-Tantalum 0.015-Gallium 0.25	14.0	21.0
25	Niobium Nitride (B-1)	16.0	28.7
26	$Gd_{0.2}$-Pb-Mo_6-S_8 (Chevrel Phase)	13.9	61.0
27	V_2 (Hf, Zr) 35 a% Zr (Laves Phase C-15)	9.4	25.4
28	V_2 (Hf, Zr) 45 a% Zr (Laves Phase C-15)	9.9	27.2
29	V_2 (Hf, Zr) 50 a% Zr (Laves Phase C-15)	9.7	29.4
30	$La_{1.85}$ $Sr_{0.15}$ Cu O_{4-Y} (High Tc)	28.0[a]	27.3[c]
31	$Y_{0.4}$ $Ba_{0.6}$ Cu $O_{2.22}$ (High Tc)	61.0[b]	55.0[d]

[a]Actual Tc = 35 K; this value is the effective value. (See Fig. 3)
[b]Calculated Bc2 based on d Bc2/d T.
[c]Actual Tc = 89 K; this value is the effective value. (See Fig. 3)
[d]Calculated Bc2 based on d Bc2/d T.

The A-15 compounds and similar compounds do not have set values of T_c or B_{c2}. The value of T_c is a function of how the compounds were formed. Thus, T_c is a function of processing as well as the composition of the superconductor. Values of T_c and B_{c2} can be a function of irradiation and the formation of pinning sites.[24] In addition, for a given T_c a thin-film form of A-15 and B-1 conductors will have different values of B_{c2} depending on the direction of the magnetic induction.[25,26] If one defines $B_{c2}(0)$ as the point where bulk current carrying capacity ceases, one finds the compounds can be characterized by an equation[8] similar to Eq. (5) or a form of the WHH Theory.[27,28]

The high-T_c superconductors appear to behave more like the various compounds rather than the alloy conductors. The T_c of the high-T_c superconductor depends on how it is defined.[29,30] The only significant value in terms of a useful current-carrying superconductor is the value at which the resistance goes to zero. When one looks at a plot of T_c versus B_{c2}, one sees that the value of T_c drops significantly for small changes of B_{c2}. The T_c-versus-B_{c2} curve then goes onto another almost straight line that is much steeper than the line representing T_c versus B_{c2} at low values of B.[20] (For $La_{1.85}\ Sr_{0.15}\ Cu\ O_{4-Y}$, the zero-field T_c is 35 K.) The value at the intercept of the steep-line curve is 28 K. For $Y_{0.4}\ Ba_{0.6}\ Cu\ O_{2.22}$ the curve has an intercept T_c of 61 K when the zero-resistance T_c at zero field is 89 K. The value of $T_c(0)$ that should be used for high-T_c conductor in Eqs. (5) and (6) is the intercept of the steep part of the B_{c2}-versus-T_c curve with the B = 0 axis (see Fig. 3)

CRITICAL INDUCTION VERSUS CRITICAL TEMPERATURE FOR $Y_{0.4}Ba_{0.6}Cu\ O_{2.22}$ AND $La_{1.85}Sr_{0.15}Cu\ O_{4-y}$ HIGH Tc SUPERCONDUCTOR

Source of Data: K. Noto et al (1987)

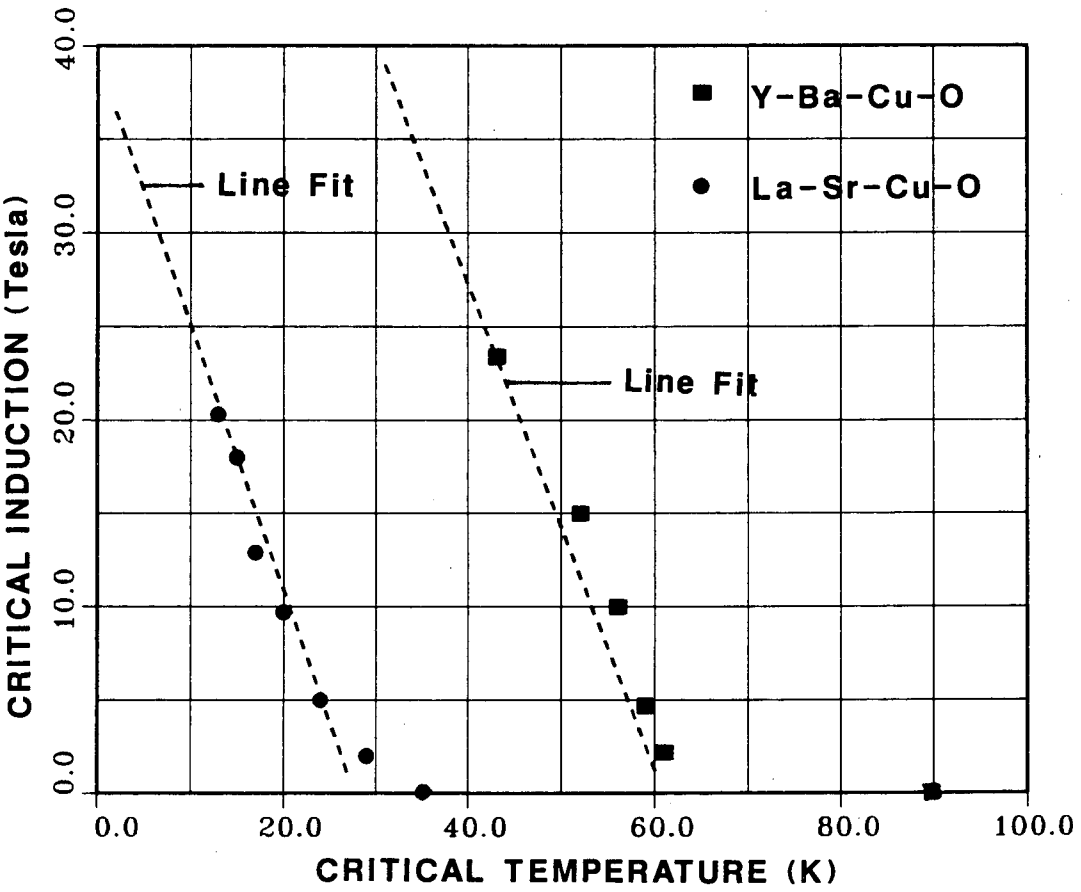

XBL 882-668

Figure 3 The change of slope of the B_{c2} versus T curve for two high T_c superconductors with zero resistivity at zero current (see Figure 2 and see Reference 20)

The J_c, B, T Surface

Once the B_{c2}-versus-T_c curve has been determined at zero critical current, a large part of the critical surface can be calculated, provided one knows the critical current versus magnetic induction at a temperature that is less than the critical temperature.

The current density in the superconductor at a given temperature T and a magnetic induction B can be calculated using the following equation:

$$J_c(T,B) = J_c(T_o,B) + \frac{dJ_c}{dT}(T - T_o) , \tag{7}$$

where T_o is the temperature for which a known curve of J versus B is given and where.

$$\frac{dJ_c(B)}{dT} = \frac{J_c(T_o,B)}{T_o - T^*} . \tag{8}$$

When Eq. (5) is used to define B_{c2} versus T at zero J:

$$T^* = (1 - B_{cR})^{\frac{1}{N}} T_c(0). \tag{9}$$

When Eqs. (6a) and (6b) are used to define B_{c2} at zero J versus T:

$$T^* = (1 - 0.6935\ B_{cR})\ T_c(0), \tag{10a}$$

when $B_{cR} \leq 0.558$, and

$$T^* = 0.9221\ (1 - B_{cR})^{0.5}\ T_c(0), \qquad (10b)$$

when $B_{cR} \geq 0.558$.

Equation (7) is valid only over the range of magnetic induction B for which $J(T_o,B)$ is given. If the value of J(T,B) calculated using the Eq. (7) is negative, then J(T,B) is zero. The key elements for calculating an accurate value of J(T,B) are the values of $B_{c2}(0)$ and $T_c(0)$ used for the material and the values of $J(T_o,B)$. Given values of $J(T_o,B)$ at more than one temperature, one can improve the values of $B_{c2}(0)$ and $T_c(0)$ used in Eqs. (5), (6) and (9).

THE TEMPERATURE DEPENDENCE OF H_{c1}, COHERENCE DISTANCE, AND PENETRATION DEPTH

The SCMAG04 computer code calculates H_{c1}, coherence distance, and penetration depth as a function of temperature. From Eqs. (5) and (6) we can see that the temperature dependence of H_{c2} is different from the temperature dependence given for Type I superconductors given by London,[31] which takes the following general form from T = 0 to T_c:

$$H_{c1}(T) = H_{c1}(0)\left[1 - \left(\frac{T}{T_c}\right)^2\right], \qquad (11)$$

where T_c is the superconductor critical temperature when $J_c = 0$ and H = 0; $H_{c1}(0)$ is the superconductor lower critical field at zero temperature; and

$T_{c1}(T)$ is the calculated lower critical field at temperature T for Nb-Ti. $B_{c1}(0)$ is typically about 0.014 T [$B_{c1}(0) = \mu_o H_{c1}(0)$]. B_{c1} for Nb_3Sn is about 0.018 T; for V_3Ga, B_{c1} is about 0.037 T.

The temperature dependence of penetration depth, given by Blaschki,[32] takes the following form:

$$\lambda(T) = \lambda o \left[1 - \left(\frac{T}{T_c}\right)^4\right]^{-1/2} + \lambda_1, \qquad (12)$$

where $\lambda(T)$ is the penetration depth at a temperature T; λo and $\lambda 1$ are penetration-depth constants; T is the temperature; and T_c is the critical temperature at zero field and current density. For Nb_3Sn, $\lambda o \simeq 102$ to 126 nm, $\lambda_1 \simeq -4$ to -8 nm and $T_c \simeq 17.7$ to 18.1 K. For Nb-46.5 Ti, $\lambda o \simeq 240$ to 250 nm, $\lambda_1 \simeq -10$ to -15 nm and $T_c \simeq 9.35$ K. Equation (11) is valid up to $T/T_c = 0.99$ for Nb_3Sn,[32] but it may not be valid up to this level for other materials.

The penetration depth for Type I material has exactly the same dependence as for Type II materials.[33] The temperature dependence of coherence distance has not appeared in the literature the author has searched. (It may be there.) The author applied the same temperature dependence to superconductor coherence distance in the SCMAG04 program as he did for the penetration depth [see Eq. (12)], which takes the following form:

$$\xi(T) = \xi(0) \left[1 - \left(\frac{T}{T_c}\right)^4\right]^{-1/2}, \qquad (13)$$

where $\xi(0)$ is the coherence distance at $T = 0$, and $\xi(T)$ is the coherence distance at temperature T. Clearly there is an upper limit on the coherence distance. This limit is probably dictated by the normal-state coherence distance for the superconductor.

In most cases, the temperature dependence of λ and ξ is not of much concern. These values only come into play when they are a significant fraction of the superconducting filament radius (or the thickness of the layer of superconductor for material reacted onto the surface of a filament). In general, when λ and ξ approach the superconductor thickness other types of effects come into play that make the use of λ and ξ of little practical value. (In niobium titanium when the filament size approaches λ or ξ, there is a considerable change in T_c and B_{c2}.)

CRITICAL CURRENT DENSITY AS A FUNCTION OF TEMPERATURE AND MAGNETIC INDUCTION FOR NIOBIUM TITANIUM

The calculation of the critical current density $J_c(T,B)$ at induction B and temperature T requires that one knows the $J_c(T_o,B)$, where T_o is the temperature at which critical current density is known [see Eq. (7)]. The value of J_c is often known at the boiling point of helium, 4.22 K. At a magnetic induction of about 1.0 tesla and above, the value of J_c is often known. Below 1.0 T, there are almost no valid measured data of critical current density except those taken using magnetization measurements.

The J_c Versus B at 4.2 K

The extension of measured data to high fields is usually quite easy. From a magnetic induction of about 0.6 B_{c2} to B_{c2} at the temperature for which there are data, the current-density function is nearly linear.[34] The following relationship can be used to estimate the critical current density given $J_c(B)$ at a B greater than 0.7 B_{c2}:

$$J_c(T_o,B) = J_c(T_o,B_o) \frac{B_{c2}(T_o) - B(T_o)}{B_{c2}(T_o) - B_o(T_o)} , \qquad (14)$$

where T_o is the temperature at which measured values, $J_c(B,T_o)$ are given; B_o is the highest magnetic induction at which the critical current density is known; $B_{c2}(T_o)$ is the critical magnetic induction at temperature T_o; and $J_c(T_o,B_o)$ is the critical current density at temperature T_o and magnetic induction B_o.

Most of the critical-current-density measurements are made using short-sample measurements. This technique has two serious flaws:

1) There is a size effect that comes into play. Large conductors will generate self field, which limits the current-carrying capacity of the conductor.[35] At fields below this self field limit, the measurement of J_c by short-sample methods is invalid. One can reduce the self-field limit only by reducing the size of the conductor.
2) Short sample measurements do not necessarily reflect the true J_c of the conductor. When the superconductor is well made, so that there is little or no "sausaging" of the filaments, the true J_c is quite close to that measured by short-sample measurements.

The use of magnetization data permits one to extend the measurement of J_c down to low fields. With niobium-titanium filaments 10 μm in diameter, one can calculate the value of J_c at magnetic inductions as low as 0.1 T. The relationship between magnetization and J_c is as follows for a superconductor:[36]

$$M(H) = \frac{2}{3\pi}\left(\frac{1}{r+1}\right)J_c(H)\, d_f , \qquad (15)$$

where M(H) is the magnetization as a function of H; r is the copper-to-superconductor ratio; d_f is the superconductor filament diameter; and $J_c(H)$ is the critical current density. The sign of J_c is a function of the flux-change history of the superconductor. Equation (15) is invalid unless the superconductor has been penetrated fully by a change in magnetic flux. Since J_c is a function of H, the magnetization given by Eq. (15) is based on the average value of J_c in the conductor.

Using Eq. (15), one can see that magnetization is proportional to the product of J_c and d_f. The limit to which magnetization can be used for calculating J_c is controlled by the penetration field of the filament. To calculate the critical current density, one has to use both sides of the magnetization loop, which can be are skewed by H_{c1} and similar effects. If both sides of the loop are used, the effects of the magnetization-loop skew are eliminated. The calculation of $J_c(H)$ takes the following form:

$$J_c(H) = \frac{3\pi}{4}(r+1)\left[\frac{|M^-| + |M^+|}{d_f}\right] , \qquad (16)$$

where $|M^-|$ is the absolute value of the magnetization of the negative side of the magnetization loop; $|M^+|$ is the absolute value of the magnetization on the positive side of the magnetization loop; and r and d_f have been previously defined.

To get values of J_c at fields below 0.1 T, one has to reduce the filament diameter.[37,38] Measurements of magnetization have been done on superconductors with filaments as small as 0.19 μm. At this diameter, the magnetization increases over the values measured at a filament diameter of 0°4 μm.[37] An explanation for this increase is proximity coupling between filaments that are close together. Proximity coupling increases magnetization without an increase in J_c.[39,40] In superconductors with a good copper matrix, the proximity coupling appears when the spacing between filament drops below 0.8 μm. Copper-manganese and copper-nickel matrix superconductor will not exhibit proximity coupling at filament spacings as low as 0.1 μm.

Figure 4 shows measured values of critical-current density versus magnetic induction for a modern superconductor (made in 1985). Two methods were used to measure the critical current density in this superconductor. The solid curve was based on short-sample measurements; the dashed curve was based on magnetization measurements. One can see that there is a 7 to 10 percent difference between the two curves. There is probably some sausaging in the filaments of the superconductor, so the superconductor exhibits normal behavior before all of the filaments carry J_c. From Fig. 4 one can see that the J_c at 0.1 T is over 7 times the J_c at 5 T.

A number of niobium titanium superconductors were examined to determine the ratio of low-field J_c to the J_c at 5 tesla. Figure 5 shows the reduced current density $\left[J_c(B) \text{ divided by } J_c(5T)\right]$ at 4.2 K. Table 5[11-46] presents the

Figure 4

CRITICAL CURRENT DENSITY VERSUS MAGNETIC INDUCTION FOR A NIOBIUM TITANIUM SUPERCONDUCTOR

See Reference 43

Source of Data: A. K. Ghosh (1986)

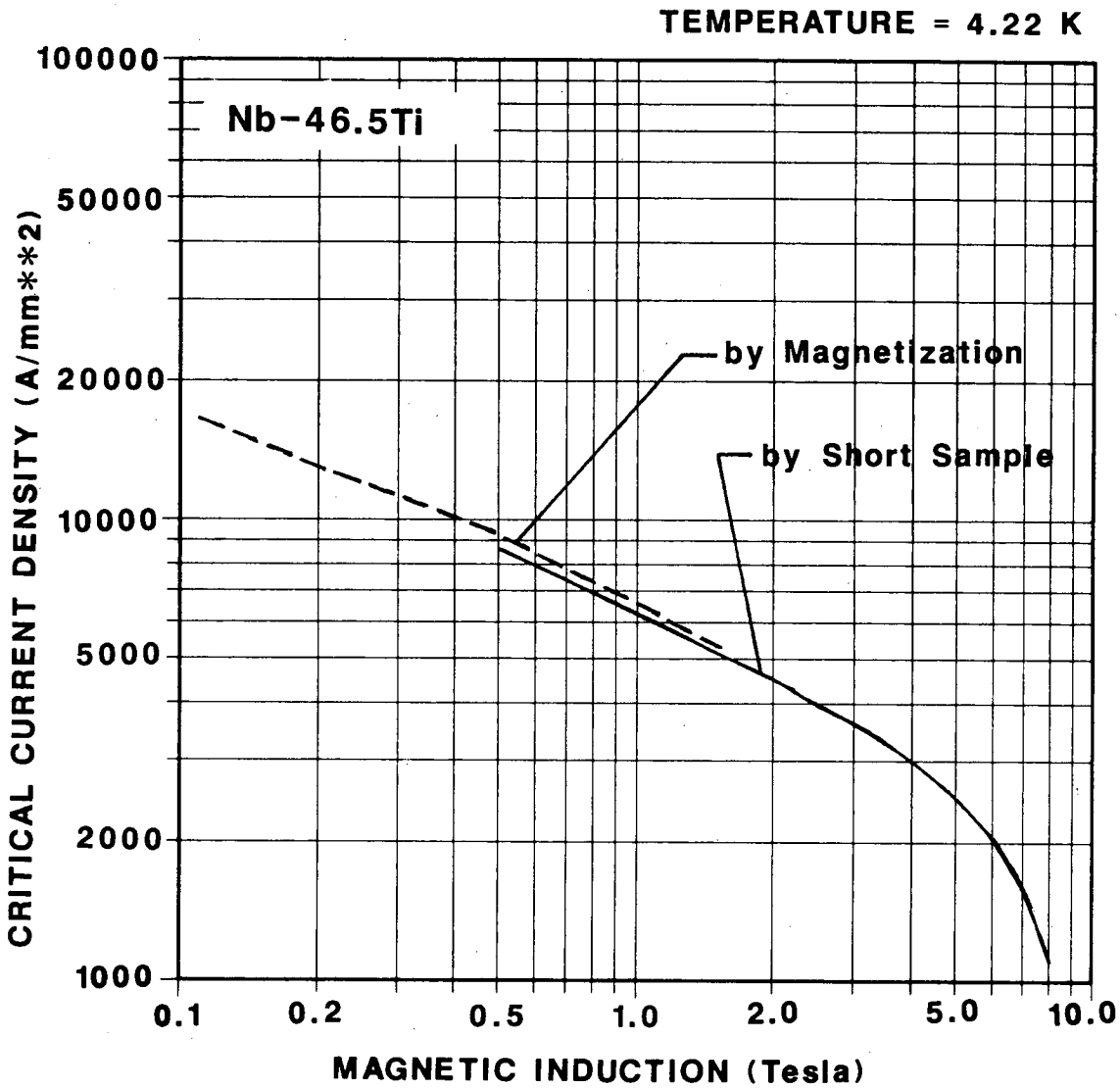

XBL 882-669

Figure 5

REDUCED CRITICAL CURRENT DENSITY VERSUS MAGNETIC INDUCTION FOR VARIOUS SAMPLES OF NIOBIUM TITANIUM

See Table 5

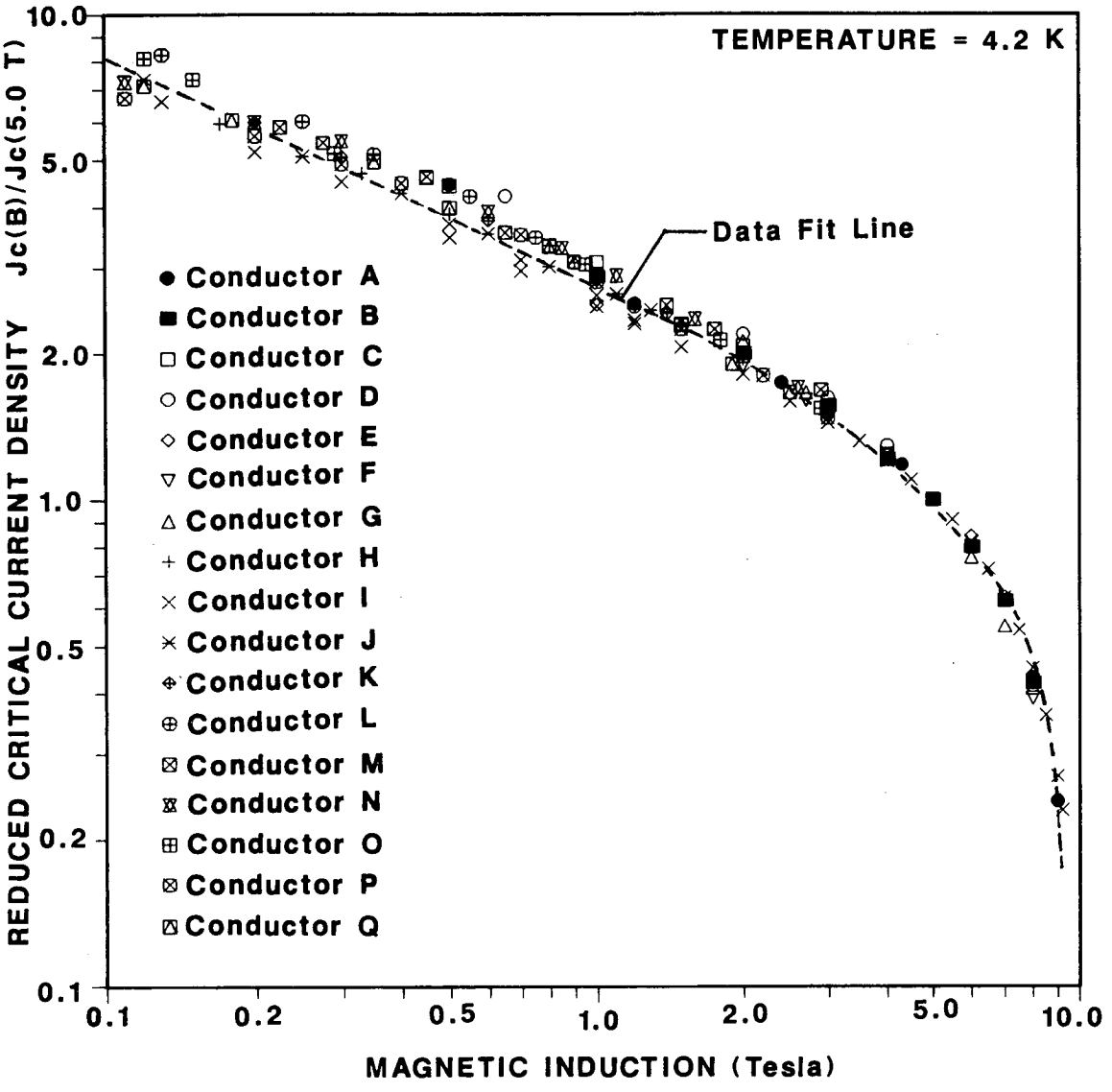

XBL 882-670

Table 5. Commercial Superconductors for which Critical-Current-Density Measurements Have Been Made (Conductor Designation Refers to Figure 5)

CONDUCTOR DESIGNATION	CONDUCTOR DESCRIPTION	YEAR MADE	FILAMENT DIAMETER (μm)	Jc (4.2 K, 5 T) (A mm^{-2})	Jc MEASUREMENT METHOD	REFERENCES
A	Nb-44.0 Ti, English (IMI)	<1972	NA	1120	Short Sample	Cond. 1, Refs. 1,2,41
B	Nb-46.5 Ti, Airco	1977	18.0	1700	Short Sample	Cond. 2, Ref. 3
C	Nb-46.5 Ti, LBL, MCA	1975	12.4	1580	Short Sample	Ref. 35
D	Nb-48.0 Ti, LBL, Supercon	1975	13.6	1580	Short Sample	Ref. 35
E	Nb-46.5 Ti, Wisconsin	1978	10.0	1930	Short Sample	Cond. 4, Ref. 4
F	Nb-50.4 Ti, Wisconsin	1978	52.0	2600	Short Sample	Cond. 6, Ref. 4
G	Nb-52.7 Ti, Wisconsin	1978	38.0	1650	Short Sample	Cond. 7, Ref. 4
H	Nb-Ti, French	<1985	1.33[a]	1680	Magnetization	Ref. 38
I	Nb-46.5 Ti, BNL-MCA 0045	1985	4.0[a]	2500	Both	Ref. 43
J	Nb-Ti, BNL-FUR 0029	1985	2.7[a]	2380	Magnetization	Ref. 43
K	Nb-46.5 Ti, BNL	1986	18.6	2025	Magnetization	Refs. 44,45
L	Nb-46.5 Ti, BNL-LBL-1	1986	8.4	2900	Magnetization	Refs. 44,46
M	Nb-46.5 Ti, FNAL-2602	1979	19.3	1970	Magnetization	Ref. 42
N	Nb-46.5 Ti, FNAL-4008	1985	8.7	2501	Magnetization	Ref. 42
O	Nb-46.5 Ti, FNAL-0274	1979	8.7	1700	Magnetization	Ref. 42
P	Nb-46.5 Ti, FNAL-2629	1979	8.7	2010	Magnetization	Ref. 42
Q	Nb-46.5 Ti, FNAL-2120	1979	8.7	2200	Magnetization	Ref. 42

[a]Proximity coupling possible, but not apparent from data.

parameters of the superconductors given in Fig. 5. It is probable that proximity coupling is not a factor with any of the data points shown in Fig. 5. Conductors A through G and I had J_c calculated from short-sample measurements. Conductors H through Q had J_c calculated from magnetization. The scatter in the data in Fig. 5 is as large as ±16 percent. It is believed that J_c at H_{c1} (about 0.011 T) is 12 to 15 times the J_c at 5 T.

The superconductors in Fig. 5 and Table 5 include both old and new conductors. Some samples of Fermilab doubler conductors are included[42]; several SSC conductors are included[44,45]; and small-filament superconductors are also included.[37,38,43] The superconductors included are, in general, good superconductors with high values of k. (In the early stages of a transition, the curve of voltage versus current can be expressed as V proportional to I to the k power.[46]) The higher the value of k, the better the superconductor. (In a good superconductor, k can exceed 80 at 5 T.)

It is surprising that various samples of niobium titanium all behave as they do in Fig. 5. The author has found that most of the earliest published data on niobium-titanium current density behave the same as the other niobium-titanium samples shown in Fig. 5. Data from M. S. Lubell[47] in 1965 and A. El Bindari in 1967[48] behave just as the data shown in Fig. 5. The author found only one early sample of niobium titanium[49] that did not fit the data in Fig. 5. That sample was one of the earliest samples of niobium titanium tested (in 1961). The sample appears to have been neither heat treated nor cold worked. The early data published in Ref. 49 probably contributed to niobium titanium not being used extensively in superconducting magnets before 1965.

Calculation of J_c for Other Values of Temperature

Figure 6 shows the calculated value of J_c as a function of B at various temperatures for the superconductor used in the Hampshire et al. measurements.[1,2] The calculations were based on measurements at 4.22 K given by M. Taylor.[41] The points shown in Fig. 6 are measured values. From Fig. 6, one can see that the measured points agree with the calculated curves within a few percent except at 1.9 and 2.2 K. (The theory is about 7 percent high at 5 T and 1.9 K.)

The theory given in this report can be applied at any temperature for which measured data exist. Figure 7 shows the theory compared to the 1.9-K data from M. Taylor. In this case, the theory underestimates J_c at the higher temperatures, although the data fit surprisingly well over almost the entire critical surface. The theory given by Eq. (7) is designed for the entire field and temperature range, unlike the theory of G. Morgan,[50] which fits only the high-field part of the $J_c(H,T)$ surface. The Morgan theory does fit the data very well over its intended range (about one percent, from the graphs the author has seen). One should ask if the poor fit at low temperatures relates to the J_c-versus-T function or if there is some fault in the data given by M. Taylor.[41]

Low-Field Temperature Dependence

Before going on to the issue of temperature dependence at low temperatures, it is useful to discuss the temperature dependence of magnetization (which is proportional to J_c times the filament diameter) at low fields.

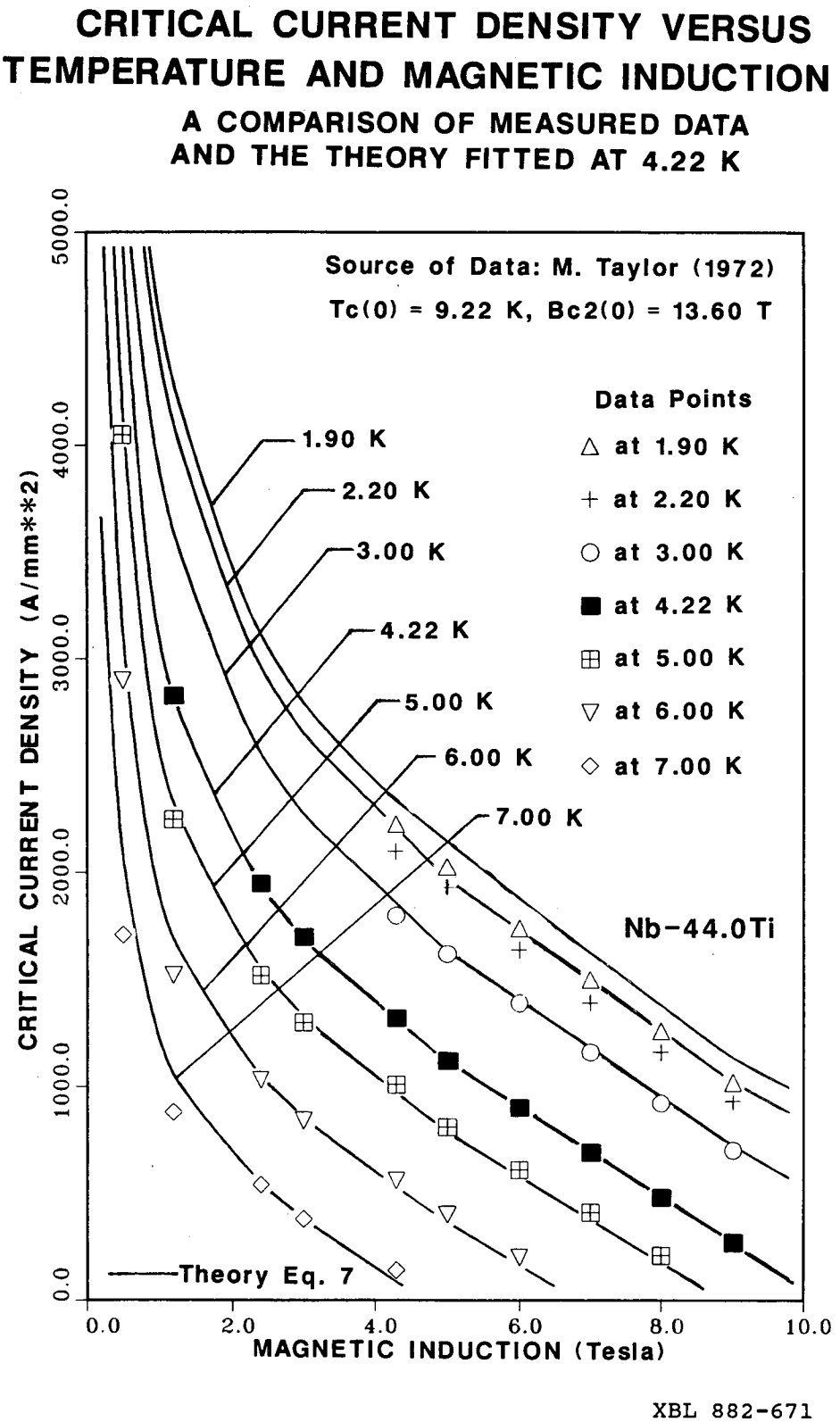

Figure 6 Critical current density as a function of magnetic induction and temperature for a Niobium -44.0 w% Titanium superconductor fitted at 4.22K with a linear temperature dependence (see References 1 and 2)

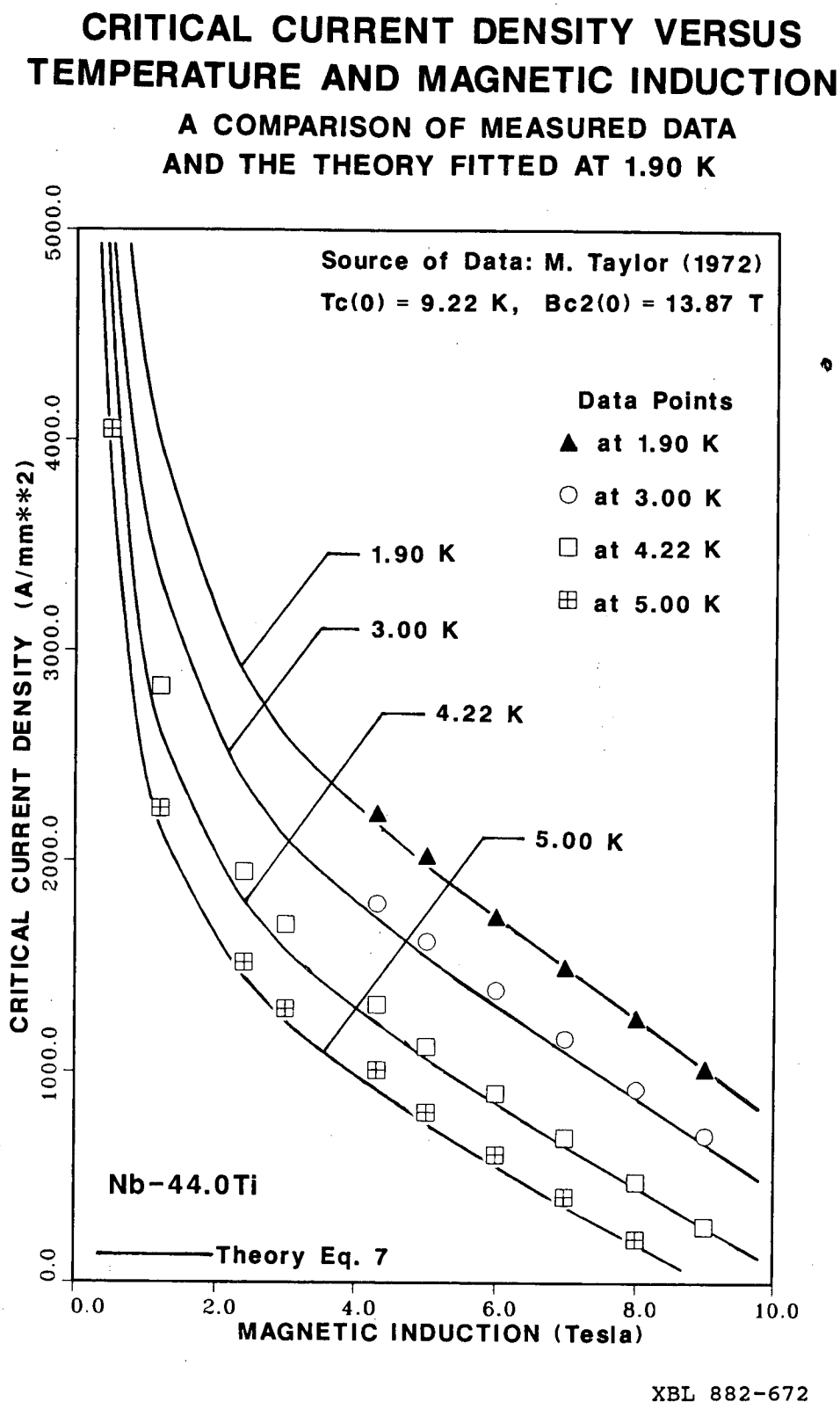

Figure 7 Critical current density as a function of magnetic induction and temperature for a Niobium -44.0% Titanium superconductor fitted at 1.90 K with a linear temperature dependence

This is of particular importance to the SSC and the kinds of schemes that can be used to correct out the magnetization-caused field errors.[51,52,53] Passive methods have been proposed for correcting the magnetization higher multipoles.[54,55] These include: 1) passive superconductor inside the coil, 2) small pieces of Mu metal or some other ferromagnetic material inside the coil, and 3) small pieces of oriented permanent-magnet material either inside or outside the coil.[55,56,57] Only the passive superconductor responds to temperature changes as the superconductor in the coil. Other methods of passive correction do not have a temperature dependence.

The theory given in Eq. (7) permits one to calculate the temperature dependence of the magnetization of niobium titanium. At 4.22 K the theory calculates for Nb-46.5 Ti (T_c = 9.35, H_{c2} = 13.6 T) the following:

$$\frac{1}{J_c}\frac{dJ_c}{dT} \approx 0.201\ K^{-1} ,$$

at a magnetic induction of 0.3 T, where T* is nearly equal to $T_c(0)$.

Measurements of the temperature dependence of the width of magnetization curves were made by Ghosh of Brookhaven National Laboratory.[58] These measurements consistently showed that dJ_c/dT divided by J_c was consistently 0.2 to 0.22 K^{-1} at magnetic inductions of 0.0 to 0.3 T. Magnet measurements by W. B. Sampson et al.[59] in 1978 indicate that the temperature dependence at 4.0 K is such that $d J_c/d T$ divided by J_c is from 0.200 to 0.208 K^{-1} at an injection magnetic induction of 0.375 T in the CBA magnets.

The injection dJ_c/dT divided by the J_c measurement shows that the simple theory given by Eq. (7) is good even at low magnetic inductions. The measured data have all been taken at a temperature above 3.5 K, where the theory given by Eq. (7) applies. Below 3.5 K the temperature dependence appears to take a different form. This temperature dependence is discussed in the next section.

The Paraboloid Temperature Fit at Temperatures Below 3.5 K

A fit was tried with some data from a paper by J.V.A. Someroski, et al.[22] that had J(T,B) data at 4.24 K and 2.5 K with a modern niobium -46.5 w% titanium superconductor [J_c(4.25 K, 5 T) = 2814 A mm^{-2}]. The theory given by Eq. (7) showed a J_c at 2.5 K that was about 10 percent higher than the measured value (see Fig. 8). Morgan of Brookhaven National Laboratory observed similar departures in modern niobium titanium at temperatures in the 2.0 to 2.5 K range at magnetic inductions from 5 to 8 T. The Morgan data showed linear temperature behavior from the critical temperature T* [see Eq. (9) or (10)] down to a temperature T', which is between 3.5 K and 4.0 K. Below low T', the J_c-versus-T dependence appears to be parabolic. This kind of behavior has also been observed to a limited extent with other superconductors.

A parabolic temperature dependence can be used to determine the J_c-versus-T behavior below about 3.5 K. The parabola should have the property that $dJ_c/dT = 0$ at $T = 0$, and dJ_c/dT must equal the linear dJ_c/dT at $T = T'$. The other boundary condition is that J_c-versus-T must be a continuous function from $T = 0$ to $T = T^*$ (see Fig. 9).

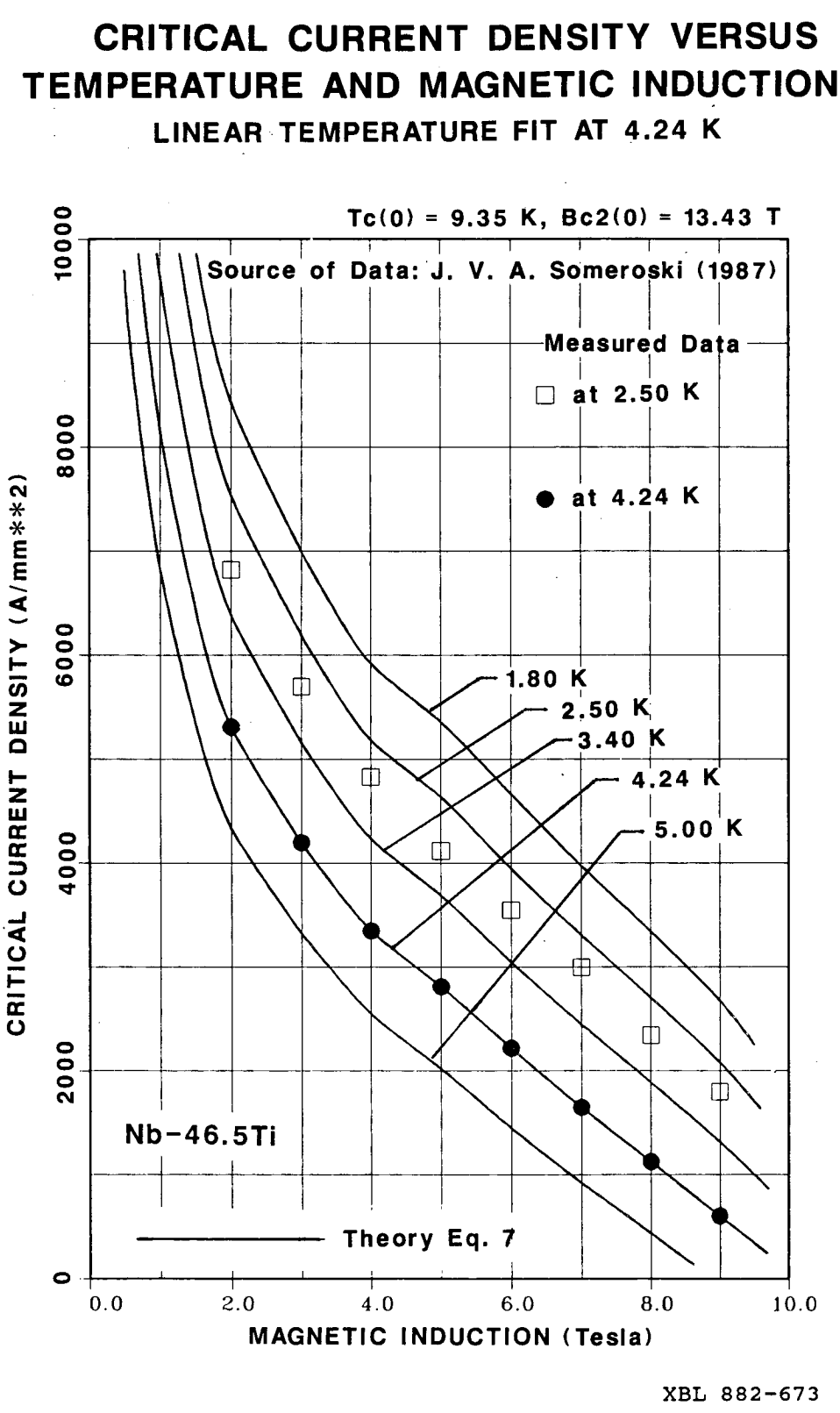

Figure 8 Critical current density as a function of magnetic induction and temperature for a modern Niobium -46.5 w% Titanium fitted at 4.24K with a linear temperature dependence (see Reference 22)

Figure 9

LINEAR PLUS PARABOLIC TEMPERATURE DEPENDENCE OF CRITICAL CURRENT DENSITY IN NIOBIUM TITANIUM

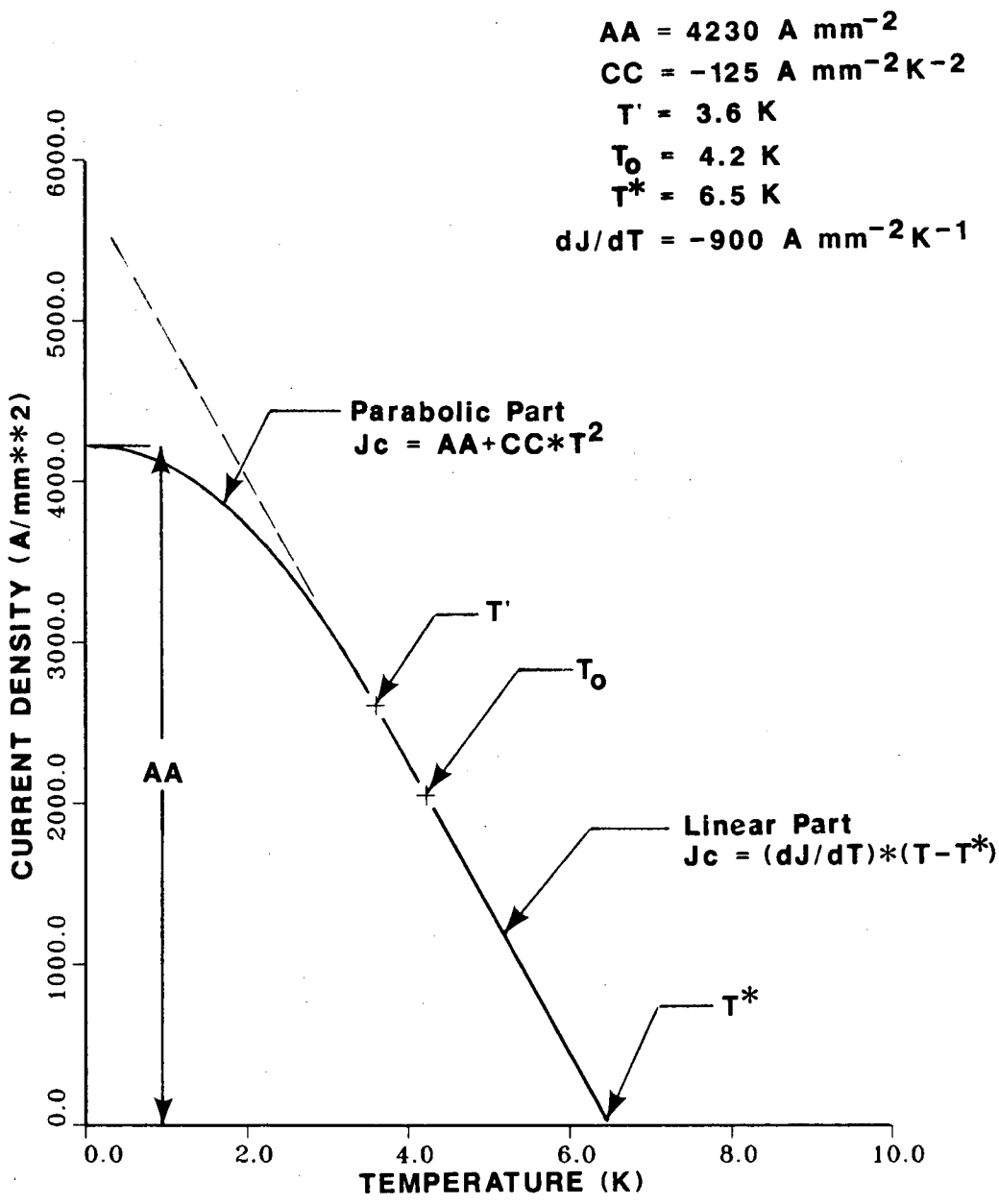

XBL 882-674

Let us look at the case where T_o is greater than T', and T is less than T'. The following set of equations now applies (at least for niobium titanium):

$$J_c(T,B) = AA - CCT^2, \tag{17}$$

where

$$AA = \frac{dJ_c}{dT}\ \frac{T'}{2} - T^* \quad , \tag{18a}$$

and

$$CC = -\frac{1}{2T'}\ \frac{dJ_c}{dT} \quad , \tag{18b}$$

where T* is determined by Eq. (9) or (10), and dJ_c/dT is determined by Eq. (8), because T_o is above T'. When T is greater than T', and T_o is greater than T', Eq. (7) is used as before. (See Figure 9 for a definition of AA, T', T* and dJ_c/dT.)

Let us look at the cases where T_o is less than T'. One can modify Eq. (17) to obtain with an estimate of the linear temperature dependence dJ_c/dT. This equation will take the following form:

$$\frac{dJ_c}{dT} = \frac{J_c(T_o,B)}{\frac{T'}{2} + \frac{T_o^2}{2T'} - T^*} \quad , \tag{19}$$

when $T_o < T'$. Use Eq. (8) when $T_o > T'$. For the case where T is also less than T', one uses Eq. (17) with the value of dJ_c/dT calculated from Eq. (19).

When $T_o < T'$ and $T > T'$, Eq. (19) is used to calculate the linear dJ_c/dT, and the following equation is used to estimate J(T,B):

$$J_c(T,B) = \frac{dJ_c}{dT} (T - T^*) , \qquad (20)$$

where dJ_c/dT is defined by Eq. (19), and T* is defined by Eqs. (9) and (10).

What value should be chosen for T'? The M. Taylor data[41] suggest that one use a value of T' = 3.4 K. However, the data of J. V. A. Someroski[22] suggest a value of T' = 3.8 K to 4.0 K. The Morgan data[50] suggest a value of T' in the 3.7-K range. If one does not have low-temperature data points to fit to, it is appropriate to use a value of T' of 0.40 $T_c(0)$. If one has some low-temperature J_c data, one can fit the data to find the best value of T'.

The effect of applying a low-temperature parabolic fit to the data given by M. Taylor is illustrated in Fig. 10. (The break temperature T' used in Fig. 10 was 3.4 K.) One can see that Fig. 10 is identical to Fig. 6 for temperatures above 3.0 K. The parabolic temperature fit was also applied to the data of Someroski (see Fig. 11). The theory used in Fig. 11 used a break temperature T' of 4.0 K.

A fit of data given by C. R. Spencer et al.[3] is shown in Figs. 12 and 13. The value of T' used in the theory was 3.6 K for both figures. Figure 12 used the Spencer data for niobium 46.5 w% titanium; Fig. 13 used the Spencer

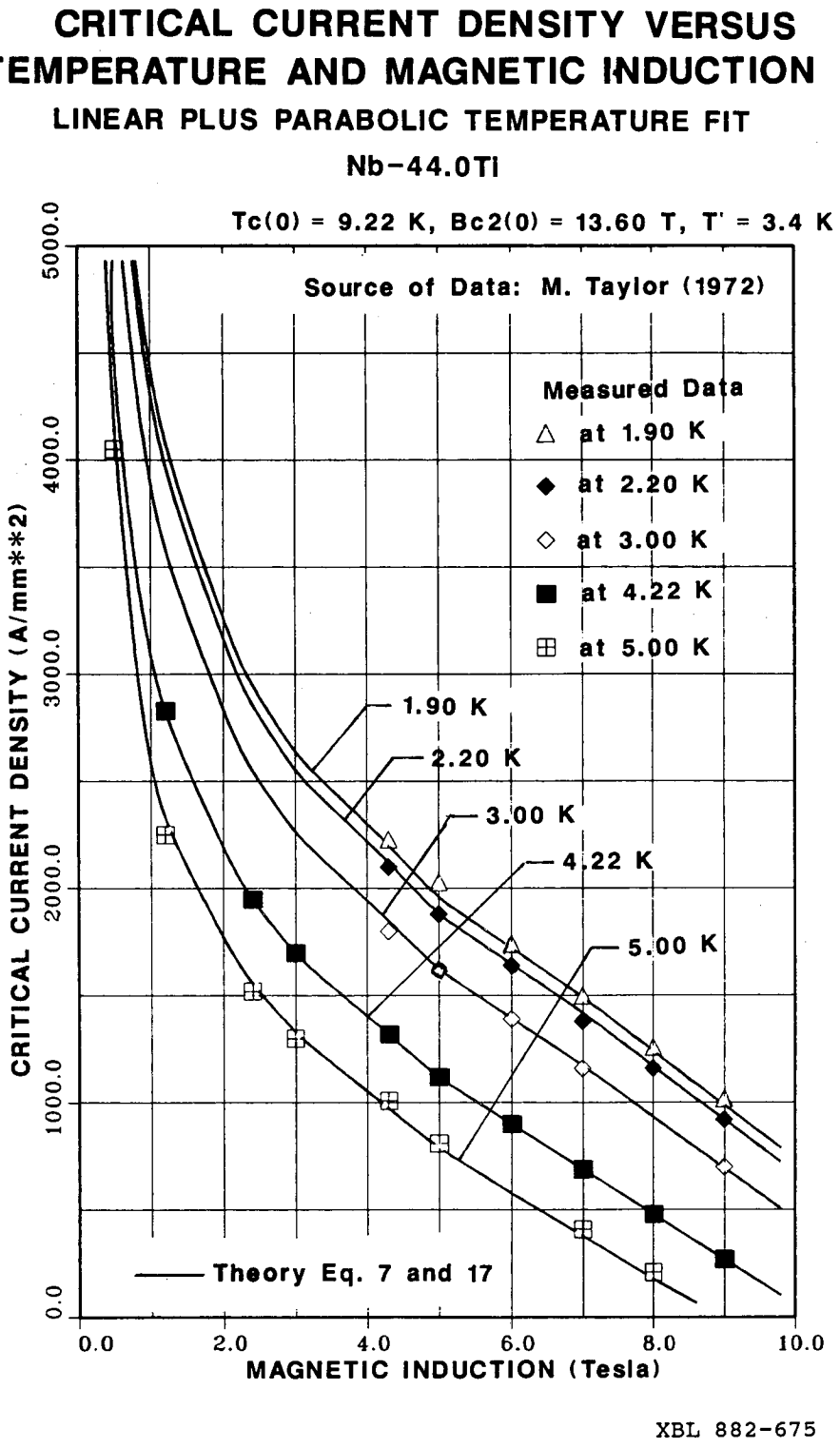

Figure 10 Critical current density as a function of magnetic induction and temperature for Niobium -44.0 w% Titanium fitted at 4.22K with a linear-parabolic temperature fit. (This is the same as the conductor in Figure 6)

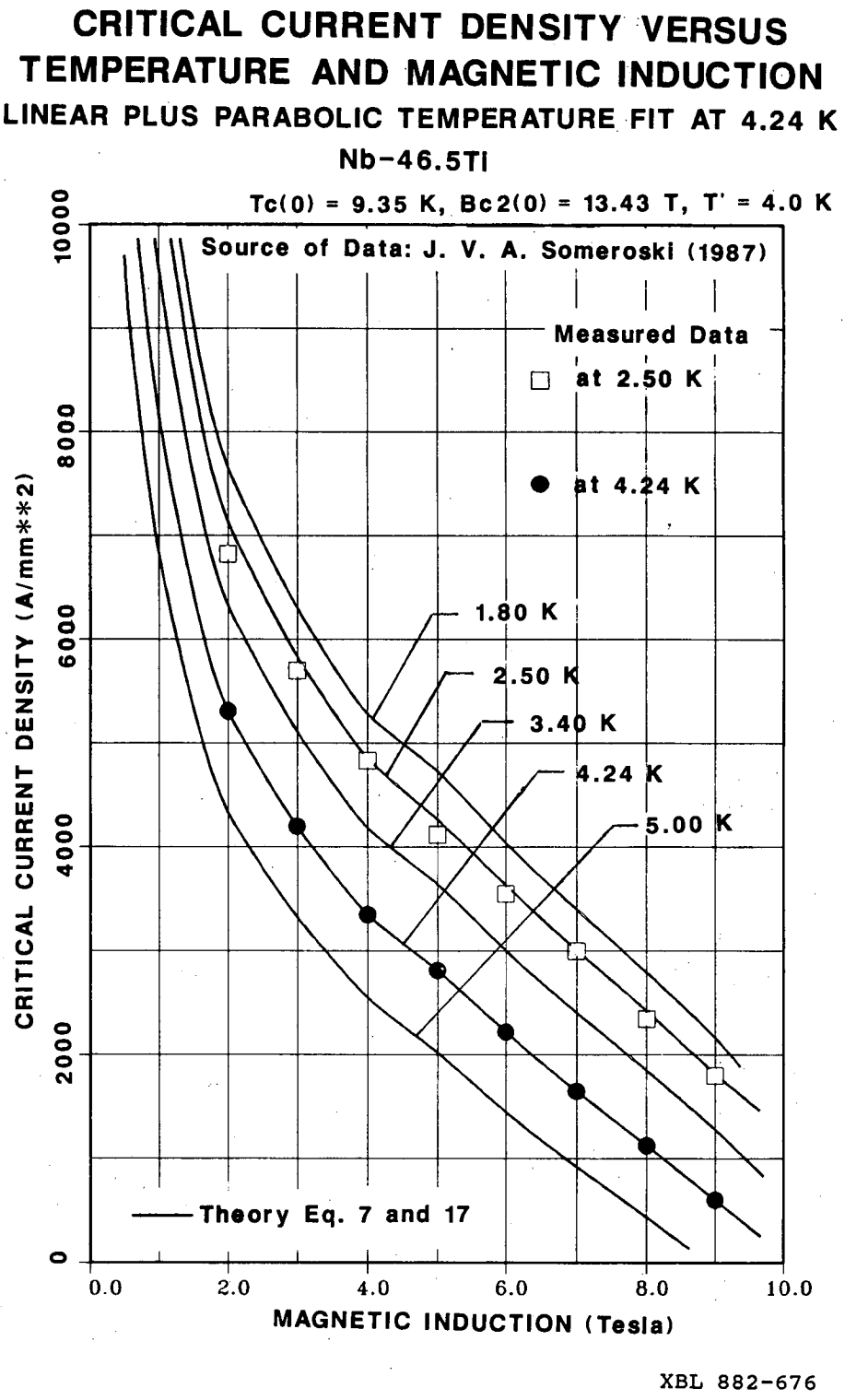

Figure 11 Critical current density as a function of magnetic induction and temperature for Niobium -46.5 w% Titanium fitted at 4.24K with a linear-parabolic temperature fit. (This is the same as the conductor in Figure 8)

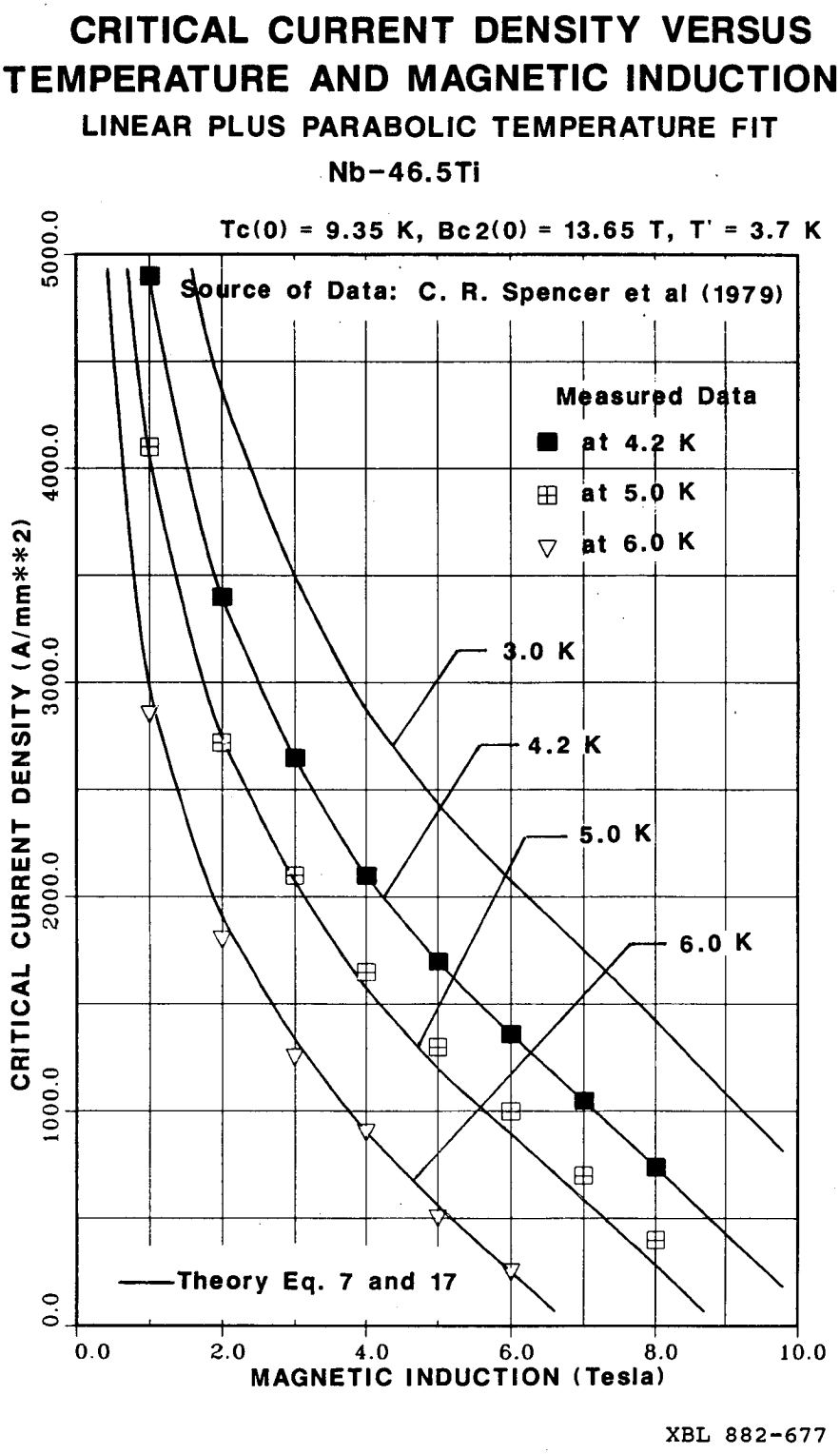

Figure 12 Critical current density as a function of magnetic induction and temperature for Niobium -46.5 w% Titanium fitted at 4.2K with a linear parabolic temperature fit (see Reference 3)

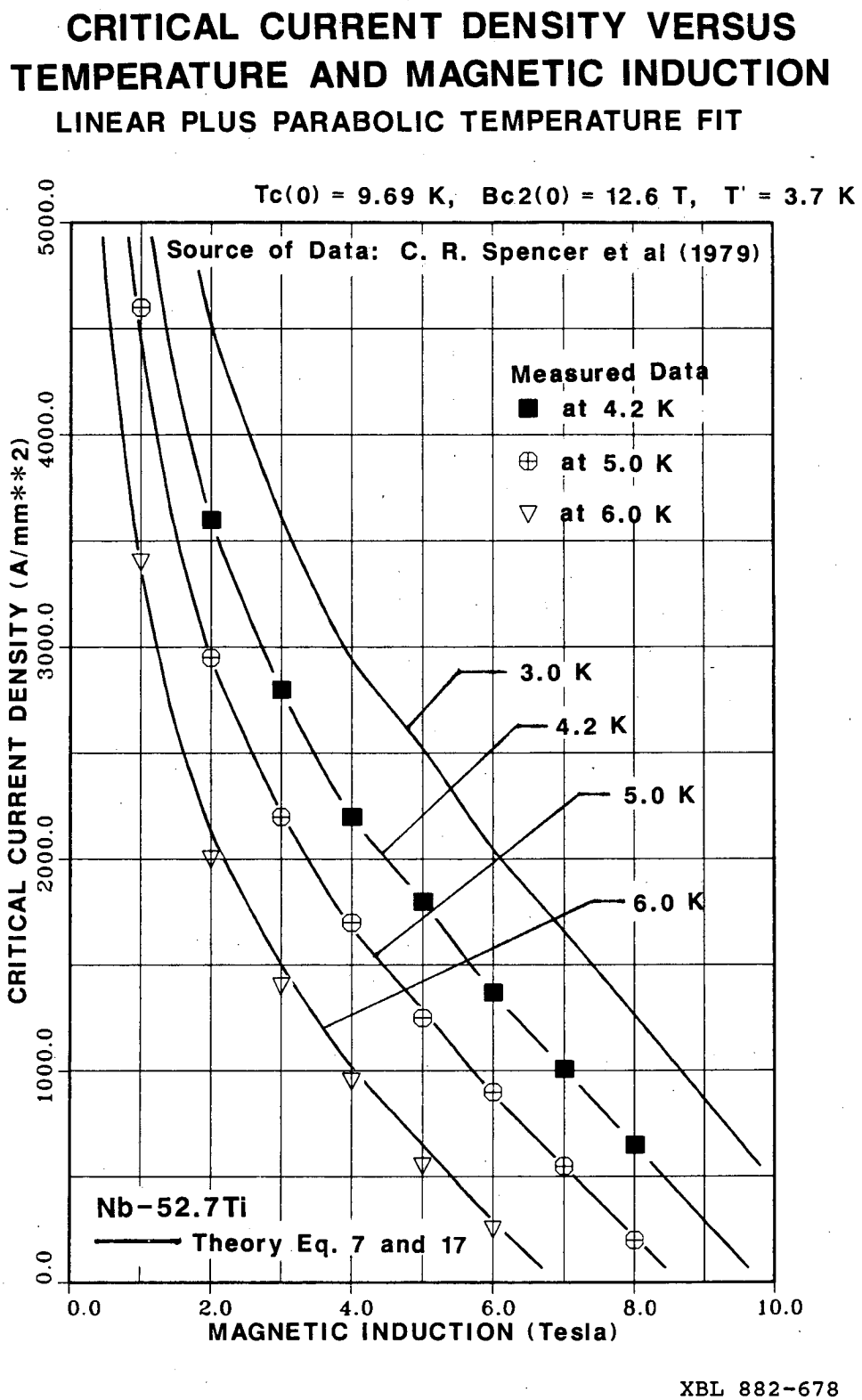

Figure 13 Critical current density as a function of magnetic induction and temperature for Niobium -52.7 w% Titanium fitted at 4.2K with a linear-parabolic temperature fit (see Reference 3)

data for niobium 52.7 w% titanium. From Figs. 12 and 13, one can see that the data fit the theory very well. (Eq. (17) was used only for the 2.0-K line.)

The use of the parabolic temperature fit for the low-temperature data permits one to calculate the critical current density for temperatures from 1.8 K to 7.0 K and magnetic inductions from 0 to about 9 T. For inductions above 9 T, a linear J_c function from 0.7 $B_{c2}(T)$ to $B_{c2}(T)$ can be applied [see Eq. (14)]. Through most of the range, one can expect to fit the theory to measurements of J_c in niobium titanium to of 2 or 3 percent.

The Effects of Strain on J_c in Niobium Titanium

Niobium titanium is relatively unaffected by stress and is ductile material that retains its ductility at low temperatures. The modulus of elasticity of usable niobium-titanium alloys varies from 7.6×10^{10} N m^{-2} for Nb-46.5 w% Ti to 7.0×10^{10} N m^{-2} for Nb-53.5 w% Ti at 300 K.[60] Niobium titanium is usually put in a copper matrix,[61] which has an elastic modulus of about 11.6×10^{10} N m^{-2}. Niobium titanium has an ultimate stress of 0.78×10^{9} N m^{-2} at 300 K. When the temperature goes down to 4.2 K, the ultimate stress goes up to 1.3×10^{9} N m^{-2}. When the niobium titanium is put into copper, the yield and ultimate stress are determined primarily by the niobium titanium.[62]

At stress levels of 6×10^{8} N m^{-2}, the critical current density is reduced to 96 percent of the critical current density at zero stress. The relationship between reduction of critical current density and stress or strain is approximately linear. After the load has been removed, the critical current density returns to 99 percent of its original value.[63] The

relationship between stress, critical current density, and niobium titanium takes the following form:

$$J_c(T,B,\sigma) = J_c(T,B,0)\ (1 - 6.7 \times 10^{-11}\ \sigma) \qquad (21)$$

where σ is the stress in the niobium titanium $J_c(T,B,0)$ is the critical current density with no stress; and $J_c(T,B,\sigma)$ is the critical current density when the wire has been stressed to a stress level of σ. Equation (21) is good up to a stress in the niobium titanium of at least 8×10^8 N m^{-2}.

CRITICAL CURRENT DENSITY AS A FUNCTION OF TEMPERATURE AND MAGNETIC INDUCTION FOR A-15 SUPERCONDUCTORS AND OTHER SUPERCONDUCTORS

The critical current density of niobium titanium can be predicted as a function of temperature and magnetic induction using the theory given in Eqs. (7) and (17). This section of the report will examine the ability of the theory to predict the critical current density versus temperature and magnetic induction for niobium zirconium, niobium tin, and other, more exotic, superconductors.

Figure 5 shows the reduced critical current density versus magnetic induction at 4.2 K for niobium titanium. Figure 14 shows reduced critical current density versus reduced magnetic induction [$B/0.5\ B_{c2}$ (4.2 K)] for niobium titanium (various samples from Fig. 5), niobium zirconium (see Ref. 6), niobium-tin ribbon (see Ref. 6), multifilament niobium tin (see Ref. 3), and multifilament vanadium gallium (see Ref. 16). The niobium

Figure 14

REDUCED CRITICAL CURRENT DENSITY VERSUS REDUCED MAGNETIC INDUCTION FOR VARIOUS MATERIALS

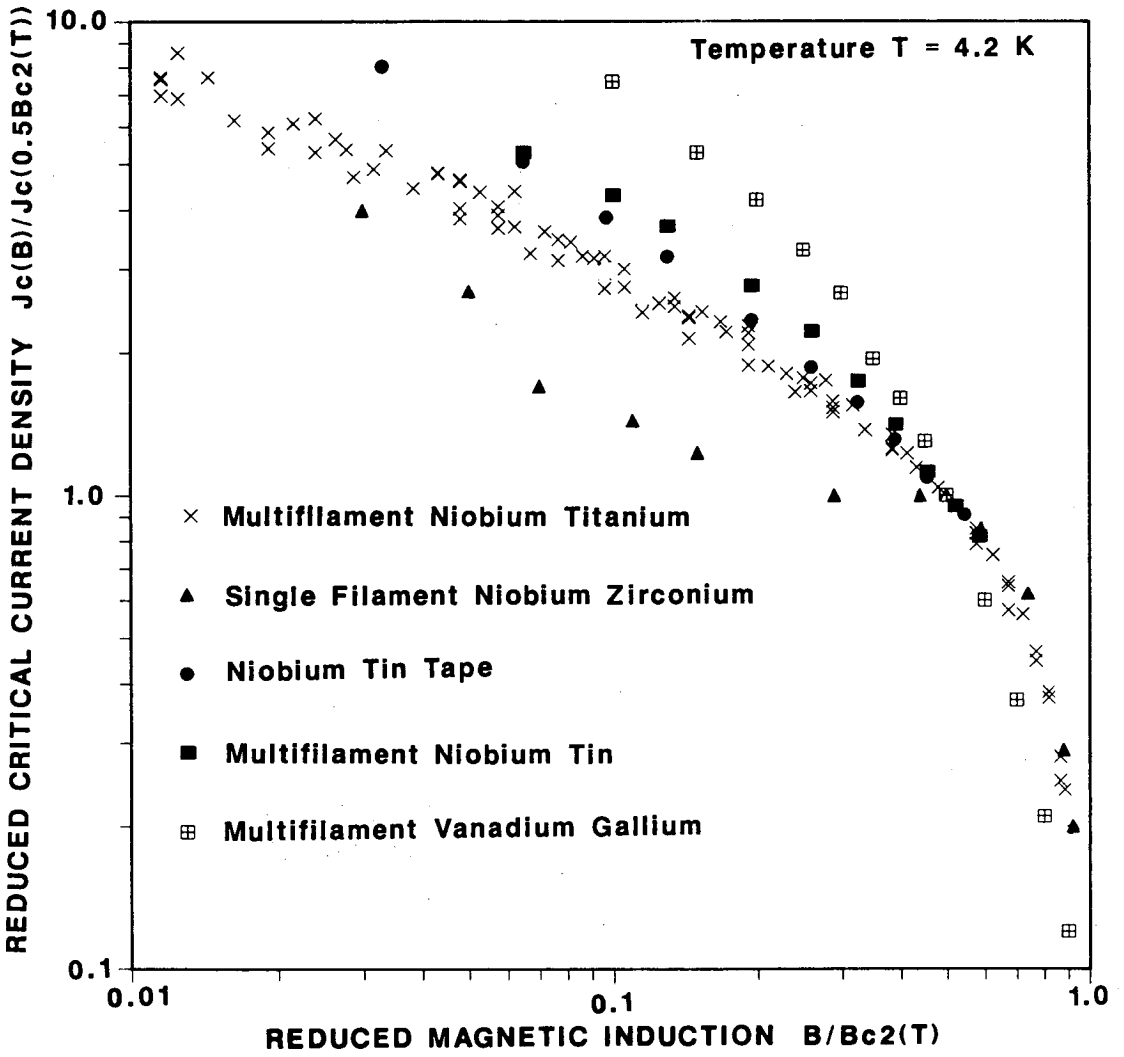

XBL 882-679

titanium data shown in Fig. 14 are the same as the data in Fig. 5 except that the induction is reduced induction. From Fig. 14 one can see that the reduced critical current density versus reduced induction for the other superconductors does not follow the data for niobium titanium.

Niobium Zirconium Data

The theory given by Eqs. (7) and (17) was fitted to the data published by Aron and Ahlgren for an alloy of niobium 25 w% zirconium in 1967.[6] The values of T_c and B_{c2} used to fit the niobium zirconium data were 10.7 K and 8.3 T. The temperature T' used was 2.8 K. The data shown in Fig. 15 were fit to measurements of critical current density at 3.0 K.

Figure 15 shows that the fit of the niobium-zirconium data to the J_c calculated by the theory is not as good as the fit of theory to the niobium-titanium data shown in the last section. The fit of the data is better at low field than at mid-range. At both 4.2 K and 5.2 K, there is a leveling off of the J_c data between 2.0 T and 4.0 T. This does not agree with the theory, which was fitted to the J_c data at 3.0 K.

Niobium Tin Data

The theory given by Eqs. (7) and (17) was fitted to critical-current-density data for an A-15 material such as niobium-tin tape and multifilamentary niobium tin in a copper and bronze matrix. The niobium-tin-tape data were taken by Aron and Ahlgren in 1967.[6] The multifilamentary-niobium-tin data were taken by S. R. Spencer et al.[3] in 1979 and P. A. Sanger et al.[64] in 1981.

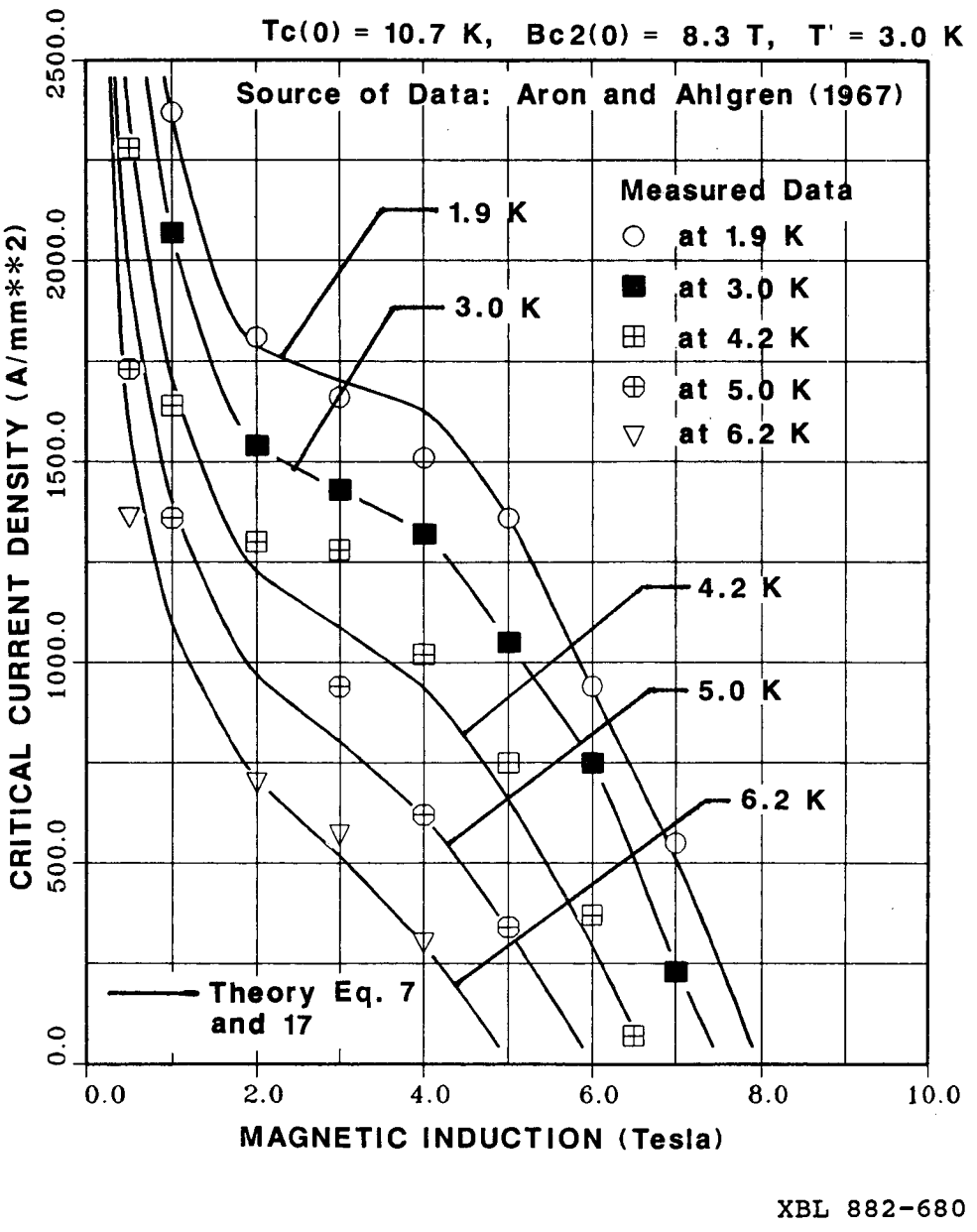

Figure 15 Critical current density as a function of magnetic induction and temperature for Niobium -25.0 w% Zirconium fitted at 4.2K with a linear-parabolic temperature fit (see Reference 6)

The niobium-tin tape was manufactured by RCA using the vapor-deposition process. This type of tape is rarely used today. The tape measured in 1967 was 2.48 mm wide with a layer of Nb_3Sn 0.0086-mm thick on both sides of the tape. The current density given in Fig. 16 is the current density in the niobium-tin layer only. The theory was fitted to the measured data at 4.2 K, (see Fig. 16). The value of $T_c(0)$ used was 17.0 K; the value of $B_{c2}(0)$ used was 16.8 T; and the value of T' used was 2.0 K. The measured data for the niobium-tin tape fit the theory quite well (to about 3 percent) except for the data at 10 K and 13 K.

The first sample of multifilamentary niobium tin consists of 2865 filaments in a bronze matrix. The section of bronze is within a copper matrix. The strand diameter is 0.69 mm. The diameter of the filaments is about 4 μm. The approximate thickness of the Nb_3Sn layer on the filaments is about 1.2 μm. The ratio of normal metal to superconductor was about 9.3 in the multifilamentary niobium tin measured by Spencer et al.[3] (The superconductor is considered to be the whole filament, which includes unreacted niobium.) Two-thirds of the normal metal is copper. Figure 17 compares theory, which was fit at 4.2 K, with measured data at various temperatures. The value of $T_c(0)$ = 16.5 K; the value $B_{c2}(0)$ = 16.8 T; and the value of T' = 1.8 K. The measured data shown in Fig. 17 fit the theory very well, even at 12 K. From the data given in Figs. 16 and 17, it appears that it is reasonable to apply Eqs. (7) and (17) to niobium tin as well as niobium titanium.

The second sample of multifilamentary niobium tin is almost the same as the sample used to generate the measured data in Fig. 17. The niobium-tin sample was made by the same manufacturer as the conductor shown in Fig. 17. The

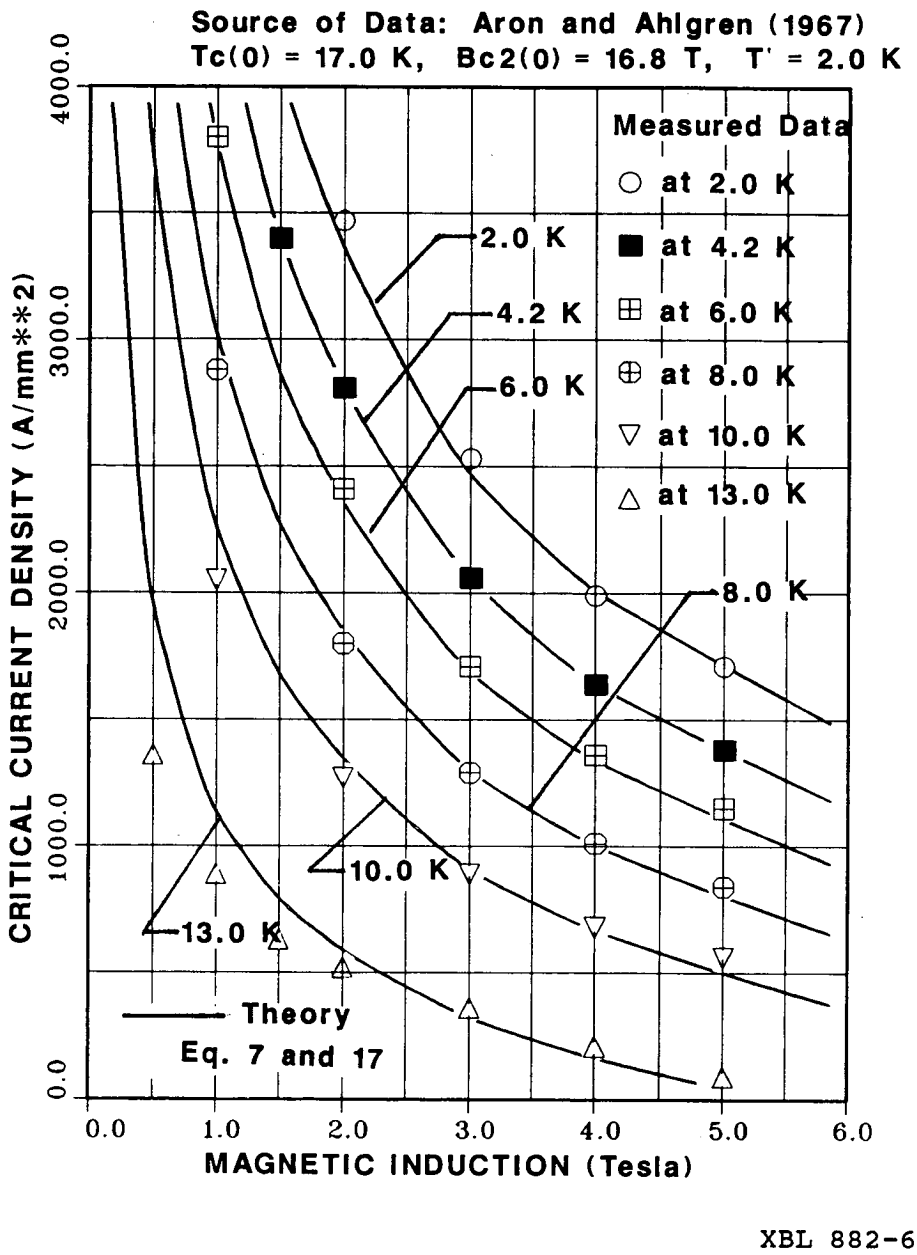

Figure 16 Critical current density as a function of magnetic induction and temperature for Niobium tin tape, an A-15 material fitted at 4.2K (see Reference 6)

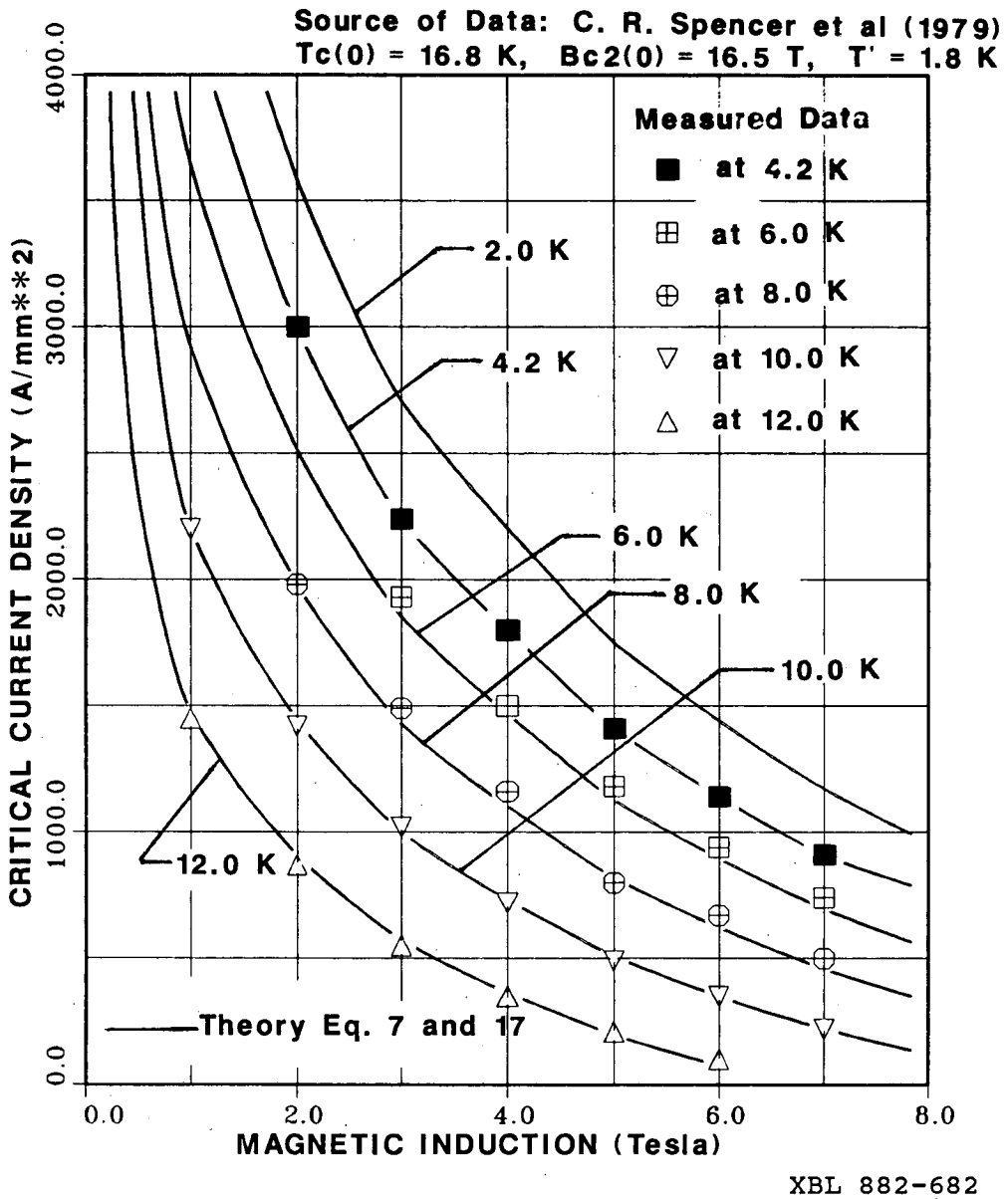

Figure 17 Critical current density as a function of magnetic induction and temperature for multifilament Niobium-Tin, an A-15 material fitted at 4.2K (see Reference 3)

difference, besides being made almost two years later, was that the second sample was optimized for high-field operation. The second AIRCO sample[64] also has 2865 filaments about 4 μm in diameter. The ratio of normal metal to superconductor ratio is also 9.3, and two-thirds of the normal metal is copper.

Figure 18 shows the critical current density versus magnetic induction and temperature for the second AIRCO sample, which was optimized for high-field operation. The measured data in Fig. 18 agree fairly well with theory except for the highest-field data. The values of $B_{c2}(0)$, $T_c(0)$, and T' are the same as for the previous sample. The value of $B_{c2}(0)$ used cuts off the low-J_c tail, which is typically found with niobium tin and other A-15 materials, and, to a lessor extent, with niobium titanium.)

Niobium tin is far more sensitive to stress and strain than is niobium titanium. The critical current density in niobium tin is sensitive to both compressive and tensile strain. When multifilamentary niobium tin is made, the niobium tin is put into compression. The compressive prestrain from the processing is typically 0.3 percent, but the exact amount of strain varies from manufacturer, to manufacturer depending on their proprietary processes. Unlike niobium titanium, which has an almost linear dependence of critical current density with strain, niobium tin has almost a quadratic dependence on strain. An approximate formula for the multifilamentary-niobium-tin critical current density with strain takes the following form, from J. Ekin's 1979 paper[65]:

$$J_c(T,B,\varepsilon_o) \approx J_c(T,B,0)\left[\frac{B_{c2}(\varepsilon_o) - B}{B_{c2}(0) - B}\right]^2 , \qquad (22)$$

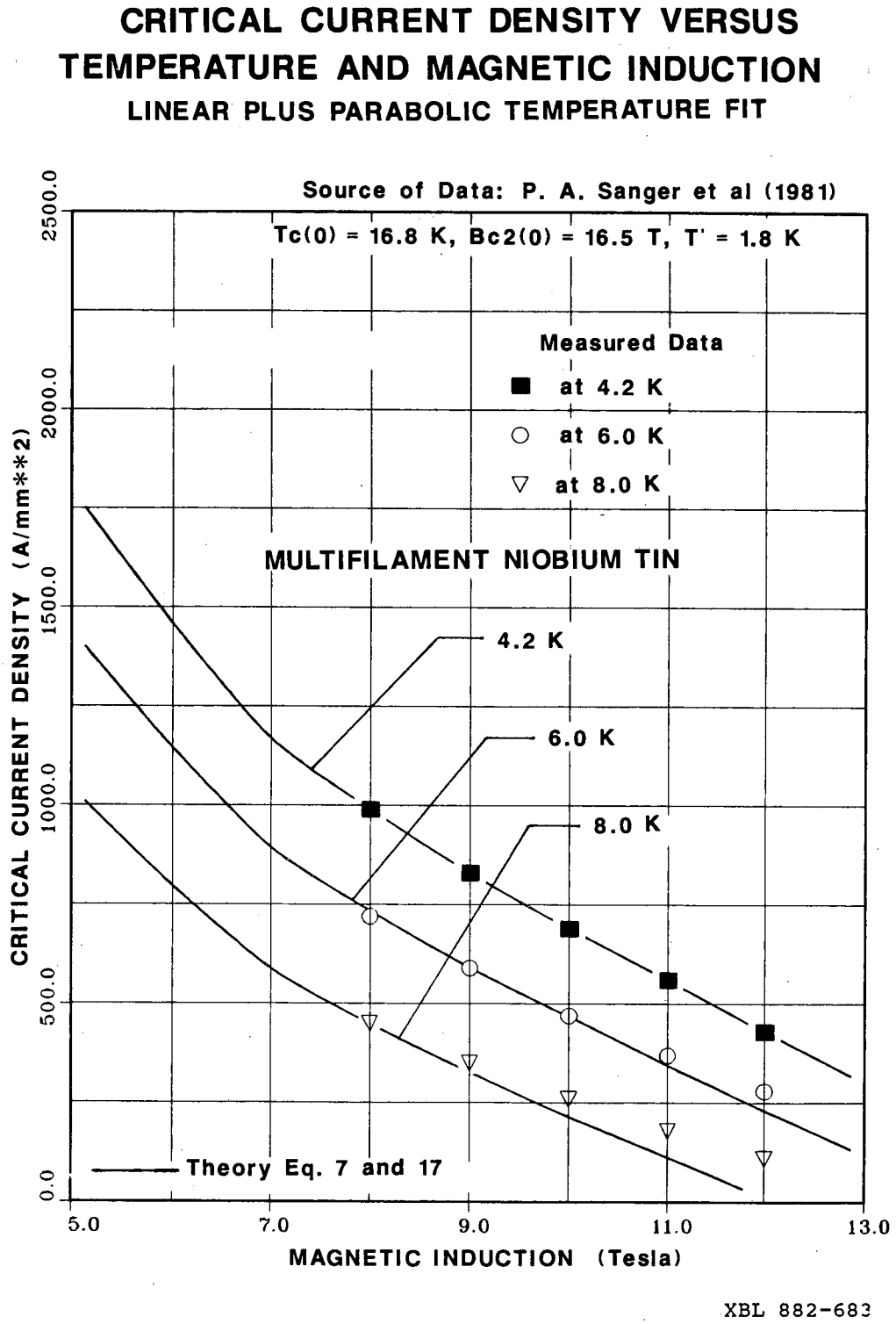

Figure 18 Critical current density as a function of magnetic induction and temperature for multifilament Niobium-tin fitted at 4.2K (see Reference 11)

where $J_c(T,B,\varepsilon_o)$ is the critical current density at temperature T, magnetic induction B, and intrinsic strain ε_o. $J_c(T,B,0)$ is the critical current density for the specimen, which has no intrinsic strain. $B_{c2}(\varepsilon_o)$ is the zero-temperature, zero-J_c upper critical induction with an intrinsic strain ε_o. $B_{c2}(0)$ is the $T = 0$, $J_c = 0$ upper critical induction with no intrinsic strain. The intrinsic strain ε_o is defined as follows:

$$\varepsilon_o = \varepsilon + \varepsilon_m \ , \tag{23a}$$

where ε_m is the compressive prestrain, which has a negative sign (ε_m can vary from -0.0015 to -0.005, depending on the conductor processing[66]), and ε is the strain put onto the wire. The value of $B_{c2}(\varepsilon_o)$ can be calculated as a function of $B_{c2}(0)$ using the following approximate expression:

$$\frac{B_{c2}(\varepsilon_o)}{B_{c2}(0)} \approx 1 - 4000\ \varepsilon_o^{\,2} \ , \tag{23b}$$

which applies up to absolute values of strain to about 0.012. At this level of strain, the conductor will lose its current-carrying capacity irreversibly. Strains as little as 0.8 percent will result in a permanent loss of current-carrying capacity. A niobium-tin multifilament conductor will undergo plastic deformation at strains of 0.3 to 0.4 percent.[67]

J. Ekin, in his 1981 paper,[68] presented a more-general form of the equation for the strain effects on critical current density, as follows:

$$J_c(T,B,\varepsilon_o) = J_c(T,B,0)\left(\frac{B^*_{c2}(\varepsilon)}{B^*_{c2m}}\right)^{k-p}\left(\frac{1 - B/B^*_{c2}(\varepsilon)}{1 - B/B^*_{c2m}}\right)^{q}, \quad (24)$$

where $J_c(T,T,\varepsilon_o)$ and $J_c(T,B,0)$ have been previously defined, and where

$$\frac{B^*_{c2}(\varepsilon)}{B^*_{c2m}} = 1 - a(\varepsilon_o)^u \quad . \quad (24a)$$

The values of k, p, q, u, and a are defined for niobium titanium, niobium tin, and vanadium gallium in Table 6. Note: The value of a depends on the sign of the strain (a minus strain is compressive; a plus strain is tensile).

Other Superconductors

The author looked at five other superconductors. Three are characterized by their not fitting Eq. (6) for the value of reduced magnetic field versus reduced temperature. Equation (5) was used to calculate B_{cR} as a function of T_{cR}. Each of these three conductors has a different value of N.

Niobium titanium tin is a slightly impure form of niobium tin that consists of one atomic percent of titanium alloyed with niobium, which is then reacted with tin to form an A-15 compound. Data between 8 T and 15 T by S. Murase et al.[69] were fit to the theory given by Eqs. (7) and (17). The value of N = 1.7 was used to obtain the reduced critical field versus the reduced temperature. The values $T_c(0)$ = 17.3 K, $B_{c2}(0)$ = 19.3 T, and T' = 1.7 K were used in the theory. Figure 19 was fitted to the measured data at 4.22 K. The experimental data at 2.13, 2.99, and 3.50 K fit the theory quite well over

Table 6. The Values of the Exponents k, p, q, and u and Values of a and B^*_{c2m} for Various Superconductors[a]

	Nb-Ti	Nb_3Sn	V_3Ga
k	4.0	1.0	1.4
p	0.66	0.56	0.42
q	0.69	2.0	1.0
u	1.7	1.7	1.7
a $\varepsilon_O < 0$	--	900	450
a $\varepsilon_O > 0$	23	1250	650
B^*_{c2m} at 4.2 K	10.5 T	22.0 T	21.2 T

[a]See Eqs. (24) and (24a) and Ref. 66.

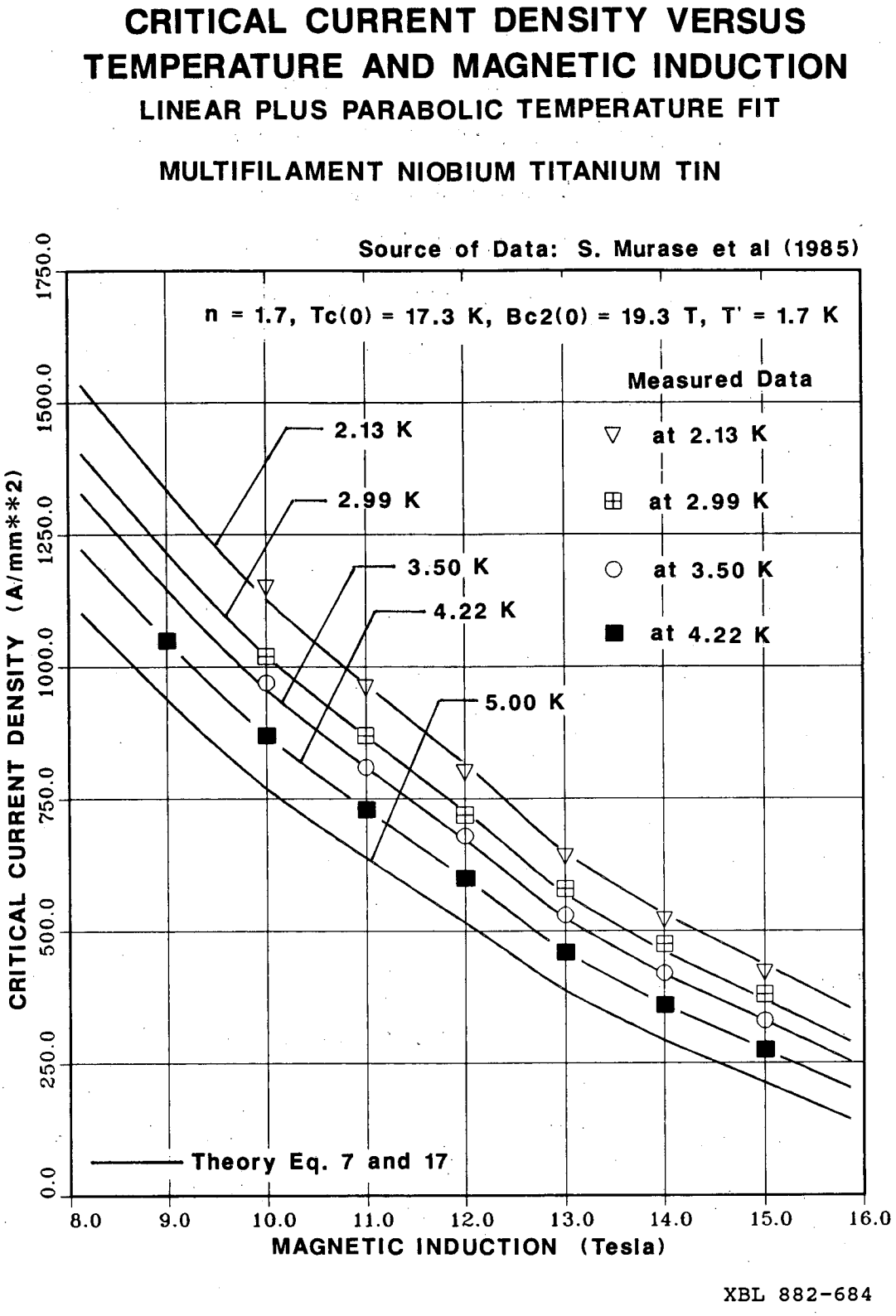

Figure 19 Critical current density as a function of magnetic induction and temperature for multifilament Niobium-Titanium-Tin, an A-15 material fitted at 4.22K (see Reference 69)

the range shown in Fig. 19. The reduction of J_c with strain for niobium titanium tin is similar to that of niobium tin.

Niobium tantalum tin is an alloy of niobium 7.5 w% tantalum that has been reacted with tin to form an A-15 compound. Data between 6 and 16 T by D. P. Hampshire et al.[13] were fit to the theory given by Eqs. (7) and (17). The value of N = 1.2 was used to generate the curve of reduced critical field versus the reduced critical temperature. $T_c(0)$ = 15.8 K, $B_{c2}(0)$ = 24.0 T, and T' = 3.7 were used to generate the theoretical values of critical current density. The theory and measured data are shown in Fig. 20. The theory fits the measured data quite well except for the 10-K data. It is interesting to note that the stated value of $B_{c2}(0)$ is 30 T. This value does not apply except out on the tail of the J_c-versus-B data. The theoretical curves shown in Fig. 20 are probably not valid at the highest temperatures or fields. The reduction of J_c with strain for niobium tantalum tin is similar to that of niobium tin.

A Laves-phase C-15 structure compound was fit to the theory. The vanadium/zirconium-45-atomic-percent hafnium [V_2(Zr-Hf)] material has an upper critical induction of 27.2 T, were the value of T_c is scarcely higher than that of niobium titanium ($T_c(0)$ = 9.9 T with $B_{c2}(0)$ = 27.2 T). The data published by K. Inoue et al.,[19] was used with a value of N = 1.7 to get a value of reduced critical field versus reduced critical temperature. The theory given by Eqs. (7) and (17) used T' = 1.7 K to fit the data. Figure 21 shows a fit of theory and measured data for T = 1.8 K, 3.1 K, and 4.2 K over a range of inductions from 4.0 T to 20.0 T. The fit of theory to measured data was quite good at the reduced temperature, up to an induction of 12 T. The calculated and estimated J_c values were quite close (within 10 percent) even at 20 T. The Laves-phase C-15 compounds are quite brittle, similar to

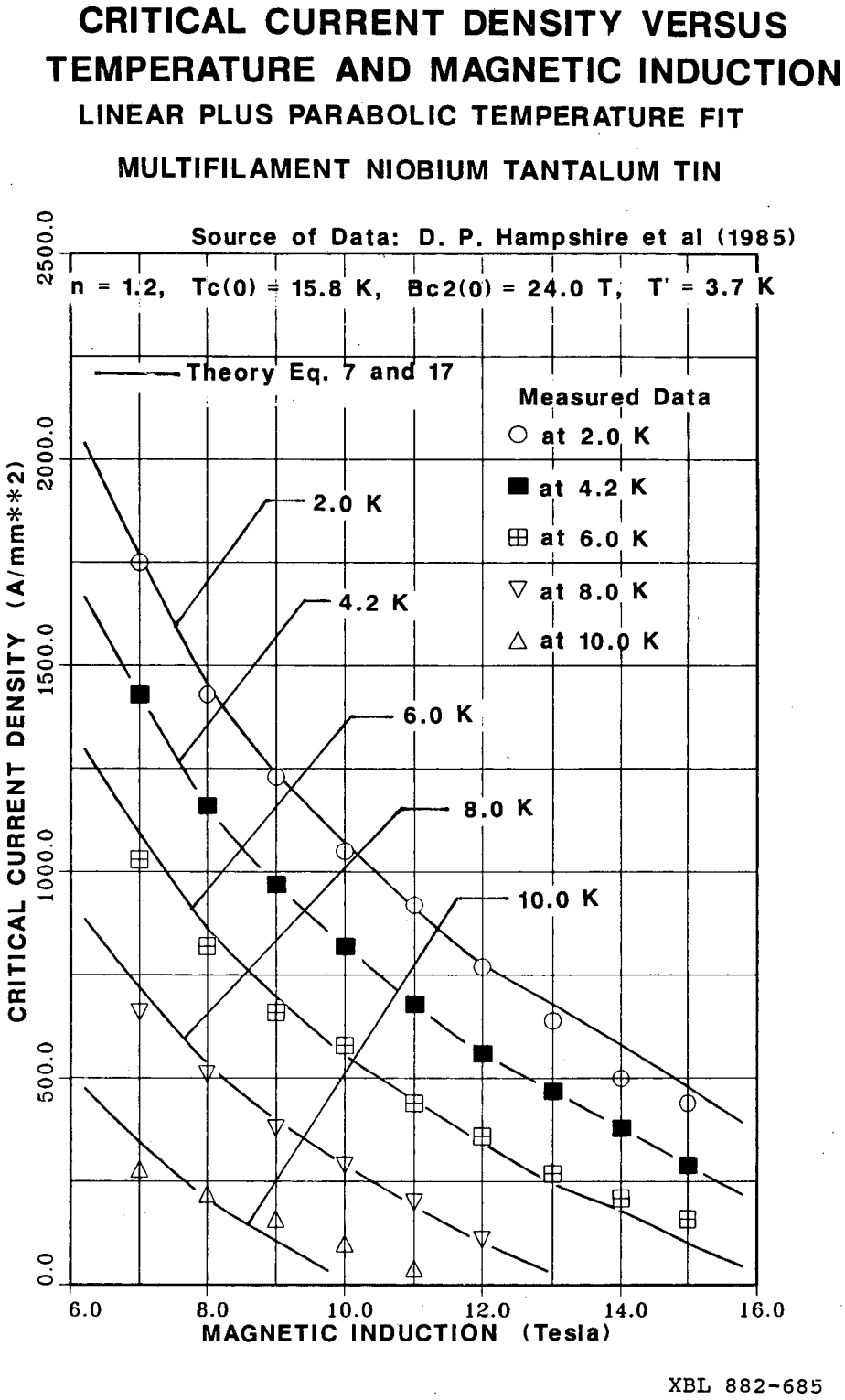

Figure 20 Critical current density as a function of magnetic induction and temperature for multifilament Niobium-Tantalum-Tin, an A-15 material fitted at 4.2K (see Reference 13)

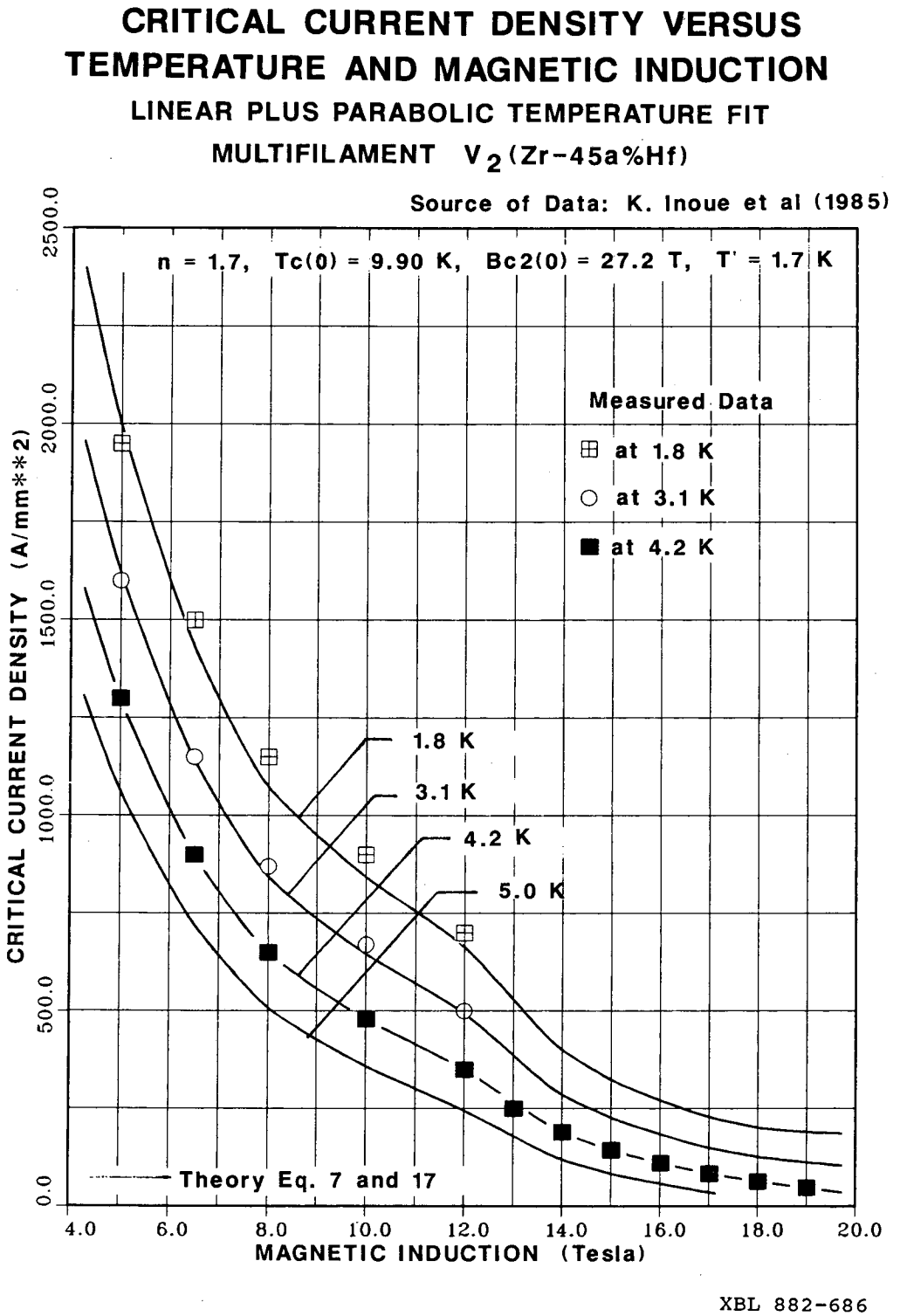

Figure 21 Critical current density as a function of magnetic induction and temperature for multifilament Vanadium-Hafnium-Zirconium, a C-15 laves phase material fitted at 4.2K (see Reference 19)

the A-15 compounds. The response to stress of the C-15 compounds is like niobium titanium up to strain levels of 0.4 percent. At these levels of strain, vanadium/zirconium-hafnium starts to break. The J_c goes down irreversibly.[70]

An attempt to fit the theory to vanadium gallium was made. There are a number of papers that give J_c-versus-B data at 4.2 K,[14,16,71,72,73,74,75] but none gives data over a range of temperatures. Another problem is that the critical current density is often given over the V_3Ga-plus-V cross section. This can yield a value an order of magnitude or more lower for the J_c than for data that are given for just the V_3Ga. Vanadium gallium can have critical current densities as high as 10^5 A mm^{-2} at 4.2 K and 2 T. At 13 T, the critical current density in such samples drops an order of magnitude. The highest-critical-current-density samples of vanadium gallium are characterized by thin layers of material, long reaction times, and rather low reaction temperatures (thus, they also have fine grain structure that enhances flux pinning in the material). One attempted fit for vanadium gallium[16] is presented in Fig. 22. The fitting parameters used are N = 2.2, $T_c(0)$ = 15.5 K, $B_{c2}(0)$ = 21.8 T, and T' = 3.7 (T' is not a factor in the calculation), and the data fitted were at 11 K. The fit is not very good because virtually all of the data are in the nonlinear tail for V_3Ga. A much-better fit for vanadium gallium[73] is shown in Fig. 23. The sample used the same values of N, $T_c(0)$, and T' as the previous case, but the value of $B_{c2}(0)$ used was 22.6 T. The fit occurred for 4.2 K in a range of magnetic inductions from 16 T to 21 T.

Niobium silicon from the data of C. L. H. Thieme et al.[76] was fitted to the theory given by Eq. (7). Values of $B_{c2}(0)$ = 26.2 T, $T_c(0)$ = 17.7 K, and N = 1.6 were used to fit data from B = 18.3 to 22.9 T and T = 2.5 to

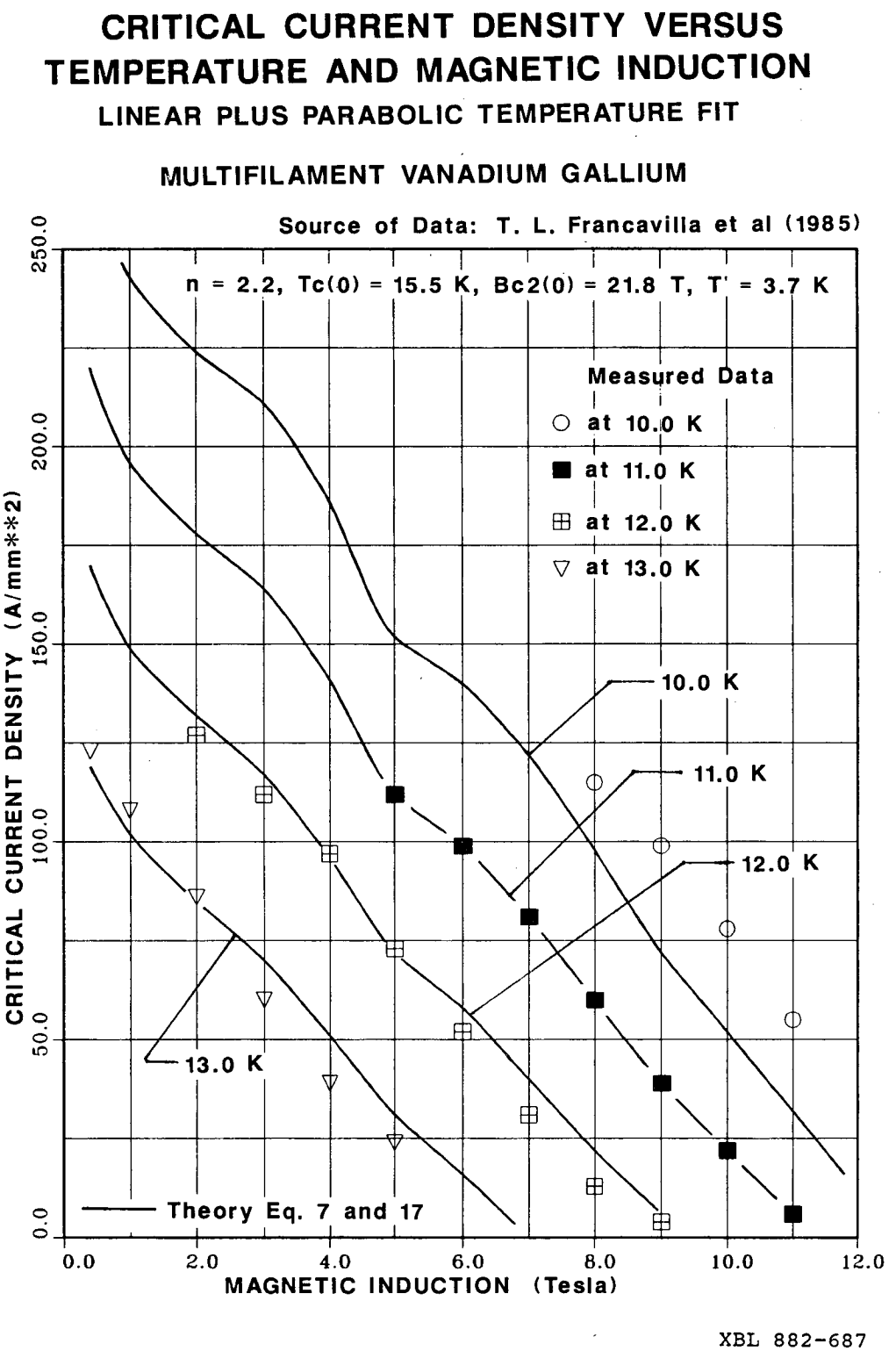

Figure 22 Critical current density as a function of magnetic induction and temperature for multifilament Vanadium Gallium, an A-15 material fitted at 11.0K (see Reference 16)

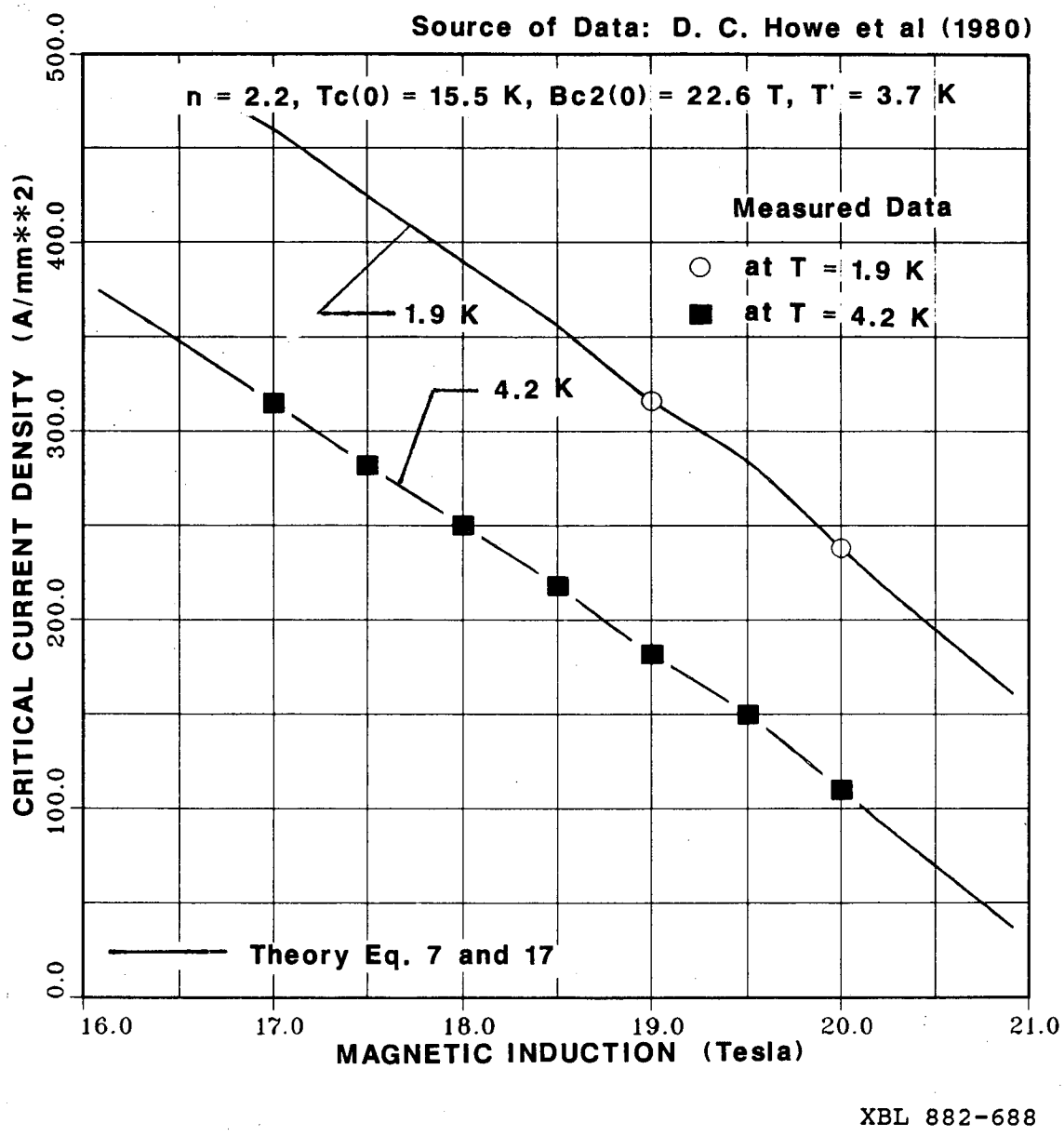

Figure 23 Critical Current density as a function of magnetic induction and temperature for multifilament Vanadium Gallium fitted at 4.2K (see Reference 71)

4.2 K, based on the measured values of J_c at T = 4.2 K. The results were disappointing because the fit was off as much as 28 percent. These data are not presented graphically.

CONCLUDING COMMENTS

Many superconducting materials are well behaved in terms of the prediction of their J_c as a function of T and B given $T_c(0)$, $B_{c2}(0)$, and some measured data points at some temperature T_o (e.g., 4.2 K). A relatively simple linear theory can be used to predict J_c for temperatures above 4.2 K for both niobium titanium and niobium tin given J_c-versus-B data at 4.2 K, $T_c(0)$, and $B_{c2}(0)$. Below some temperature T', which is about 3.7 K for niobium titanium and 1.7 K for niobium tin, the fitting theory is a little more complicated in that a parabolic temperature fit is required below T'.

The theory works very well for both niobium titanium and niobium tin. Since both superconductors are important for use in magnets, the temperature-fitting equations have been incorporated in computer codes that use the J_c of the superconductor. It has been observed that the current density of niobium titanium at 4.2 K divided by the current density at 5.0 T and 4.2 K as a function of magnetic induction lies along a line (see Fig. 5). The scatter of measured data about this line is no more than 15 percent. (There appears to be a similar relationship for niobium-tin J_c data, which the author is still collecting.) This observation suggests that if one knows the critical current density at one temperature and one magnetic induction, one knows the critical current density over the entire J_c, H_c, T_c surface.

An illustration of the reduced-equation-of-state theory used for calculating J_c in a superconductor is shown in Fig. 24, 25, and 26. Figure 24 is a three-dimensional plot of the value of J_c versus B and T for a modern niobium 46.5 w% titanium superconductor, which has a J_c at 4.2 K and 5.0 T of 3000 A mm^{-2}. The entire three dimensional surface was created from this single data point by the computer. The critical current density generated is probably accurate to $\pm$ 10 percent except at the extremes of temperature and magnetic induction. To generate the J_c values shown in Fig. 24, the following fit parameters were used: $T_c(0)$ = 9.35 K, $B_{c2}(0)$ = 13.65 T, and T' = 3.7 K. The reduced critical field as a function of reduced critical temperature was created using Eqs. (6a) and (6b). A value of J_c = 3000 A mm^{-2} at 4.2 K and 5.0 T was used along with the data fit line in Fig. 5. A contour plot of the three-dimensional surface in Fig. 24 is shown in Fig. 25. A conventional J_c-vs.-B plot is shown in Fig. 26.

ACKNOWLEDGMENTS

The author acknowledges with thanks his many conversations with A. K. Ghosh of Brookhaven National Laboratory. Much of his collected data was used to create Figs. 4, 5, and 14. The author acknowledges discussions he has had with R. Scanlan and C. Taylor of the Lawrence Berkeley Laboratory concerning superconductors. The author thanks D. C. Larbalestier of the University of Wisconsin for information gained from him during conversations at the University of Wisconsin. H. P. Hernandez, R. Scanlan and T. A. Kozman are thanked for reviewing this report.

CRITICAL CURRENT DENSITY 3 D PLOT
CRITICAL CURRENT DENSITY VERSUS
MAGNETIC INDUCTION AND TEMPERATURE

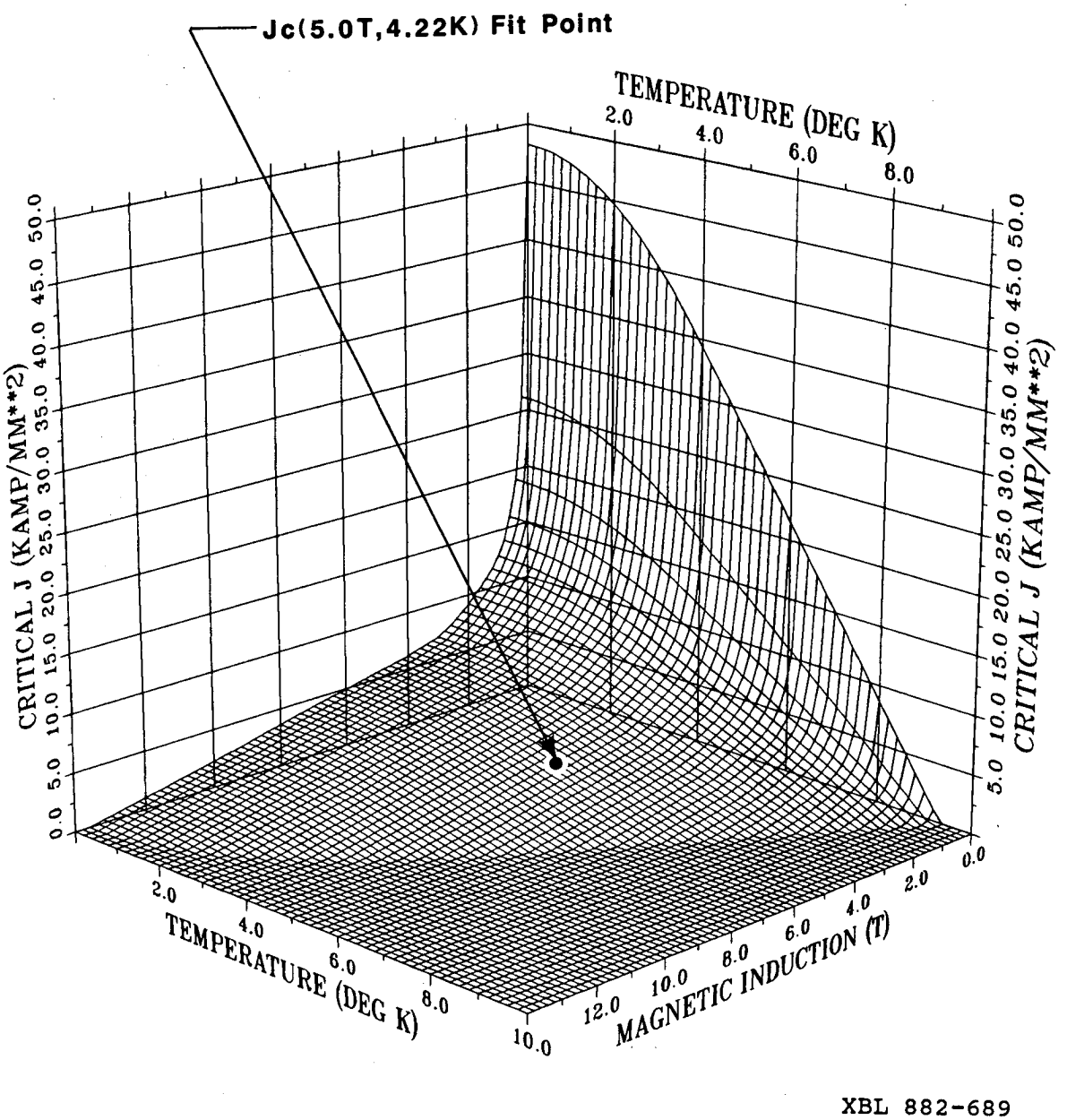

Figure 24 A three dimensional plot of the critical surface of Niobium Titanium created from a single point at 5.0 T and 4.2 K (Jc (5.0 T, 4.2 K) = 3000 A mm^{-2})

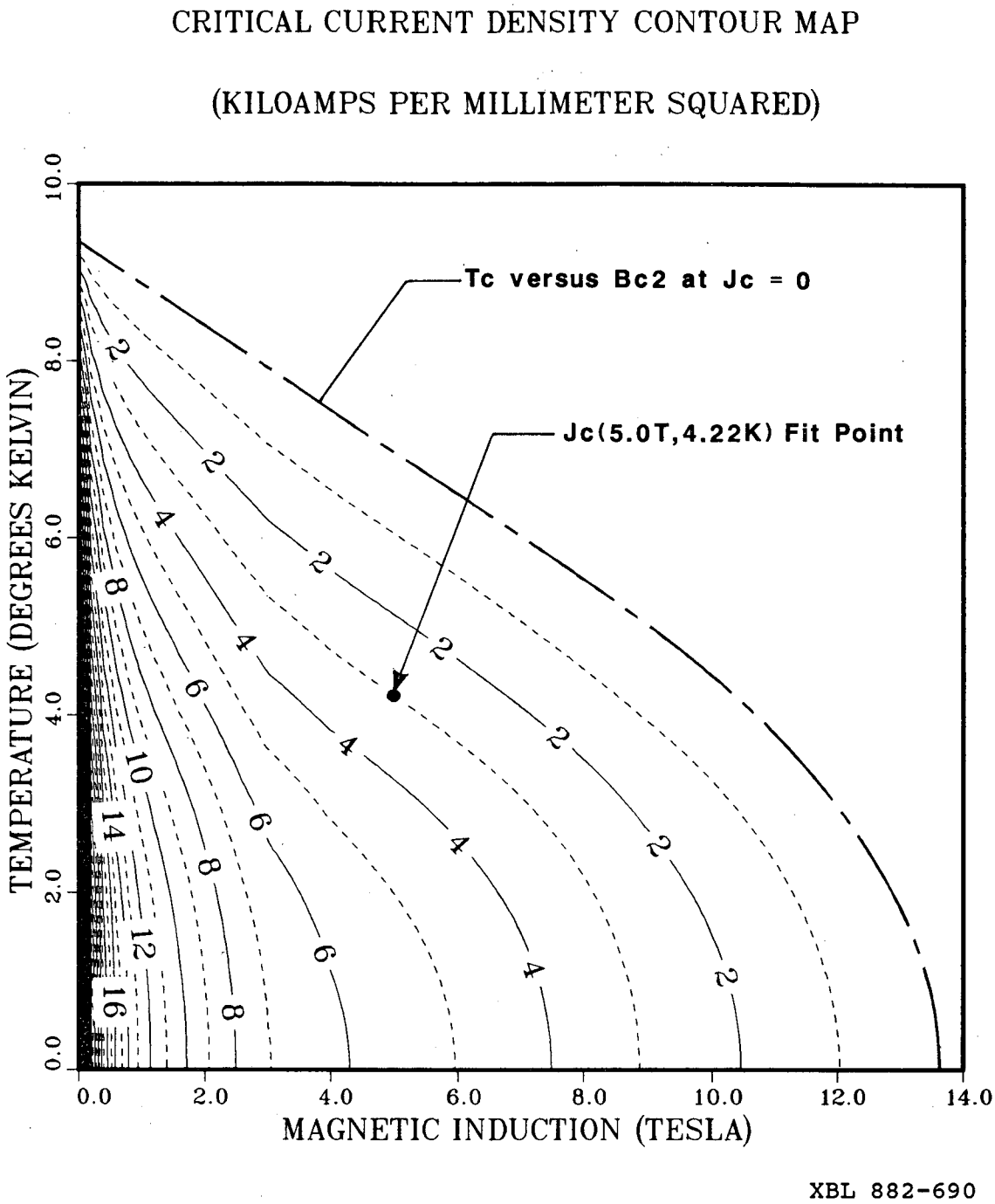

Figure 25 A contour plot of the three dimensional plot of the critical surface of Niobium Titanium shown in Figure 24.

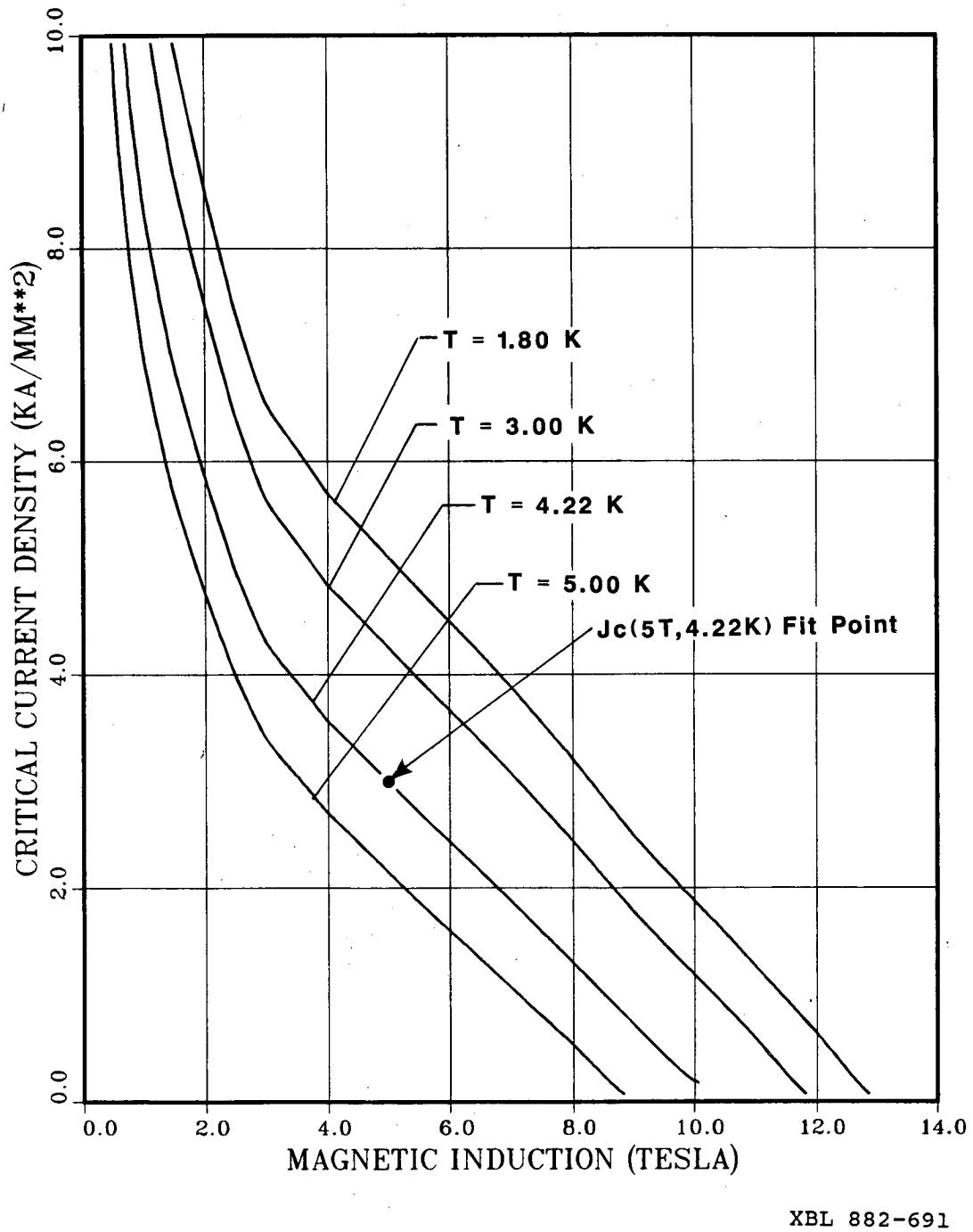

Figure 26 Critical current density as a function of magnetic induction and temperature for the Niobium Titanium shown in the three dimensional plot in Figure 24

REFERENCES

1. R. Hampshire et al., "Effect of Temperature on the Critical Current Density of Nb-44 w% Ti Alloy," Low Temperature and Electric Power, London: International Institute of Refrigeration Commission I, Annexe M69-I, pp. 251-257, 1969.

2. R. G. Hampshire and M. T. Taylor, J Phys, F, 2, p. 89, 1972.

3. C. R. Spencer et al., IEEE Transactions on Magnetics MAG-15, No. 1, p. 76, 1979.

4. K. F. Hwang and D. C. Larbalestier, IEEE Transactions on Magnetics MAG-15, No. 1, p. 400, 1979.

5. P. A. Hudson et al., IEEE Transactions on Magnetics MAG-17, No. 5, p. 1649, 1981.

6. P. R. Aron and G. W. Ahlgren, Advances in Cryogenic Engineering 13, p. 21, Plenum Press, 1967.

7. W. Schauer and F. Zimmermann, Advances in Cryogenic Engineering 26, p. 432, Plenum Press, 1980.

8. M. S. Lubell, IEEE Transactions on Magnetics MAG-19, No. 3, p. 754, 1983.

9. H. R. Segal et al., Proceedings of the 8th Symposium on the Engineering Problems of Fusion Research, IEEE Pub. No. 79CH1441-5NPS, p. 255, 1979.

10. D. C. Larbalestier, IEEE Transactions on Magnetics MAG-17, No. 5, p. 1668, 1981.

11. E. W. Seibt et al., IEEE Transactions on Magnetics MAG-17, No. 5, p. 2043, 1981.

12. D. Dew-Hughes, IEEE Transactions on Magnetics MAG-15, No. 1, p. 490, 1979.

13. D. P. Hampshire et al., IEEE Transactions on Magnetics MAG-21, No. 2, p. 289, 1985.

14. M. N. Wilson, Superconducting Magnets, Clarendon Press, Oxford, 1983.

15. B. Krevet et al., IEEE Transactions on Magnetics MAG-17, No. 5, p. 1660, 1981.

16. T. L. Francavilla et al., IEEE Transactions on Magnetics MAG-21, No. 2, p. 273, 1985.

17. P. M. Tedrow et al., IEEE Transactions on Magnetics MAG-21, No. 2, p. 1144, 1985.

18. J. R. Gavaler et al., IEEE Transactions on Magnetics MAG-19, No. 3, p. 418, 1983.

19. K. Inoue et al., IEEE Transactions on Magnetics MAG-21, No. 2, p. 467, 1985.

20. K. Noto et al., "31.1 T Hybrid Magnet and Superconducting Material Research Held at HFLSN Tohoku University," to be published in Advances in Cryogenic Engineering 34, 1987.

21. D. C. Larbalestier, IEEE Transactions on Magnetics MAG-17, No. 5, p. 1668, 1981.

22. J. V. A. Someroski et al., IEEE Transactions on Magnetics MAG-23, No. 2, p. 1629, 1987.

23. K. Yasohama et al., IEEE Transactions on Magnetics MAG-23, No. 2, p. 1728, 1987.

24. D. K. Christen et al., IEEE Transactions on Magnetics MAG-23, No. 2, p. 1014, 1987.

25. J. S. Moodera et al., IEEE Transactions on Magnetics MAG-23, No. 2, p. 1003, 1987.

26. J. E. Tkaczyk and P. M. Tedrow, IEEE Transactions on Magnetics MAG-23, No. 2, p. 948, 1987.

27. N. R. Werthamer, E. Helfand and P. C. Hohenberg, "Temperature and Purity Dependence of Superconducting Critical Field H_{c2}," Phys Rev, 147, p. 295, 1966.

28. K. Watanabe et al., IEEE Transactions on Magnetics MAG-23, No. 2, p. 1428, 1987.

29. X. Cai et al., "Experimental Evidence for Granular Superconductivity in Y-Ba-Cu-O at 100 to 160 K," Phys Rev Lett, June 29, 1987.

30. R. B. Goldfarb et al., "Evidence for Two Superconducting Components in Oxygen-Annealed Single Phase Y-Ba-Cu-O," Cryogenics 27, p. 475, September 1987.

31. F. London, Superfluids, Macroscopic Theory of Superconductivity, Dover Publications Inc., New York, 1960.

32. R. Blaschki, Advances in Cryogenic Engineering 26, p. 425, Plenum Press, New York, 1980.

33. D. Shoenberg, Superconductivity, p. 143, Cambridge University Press, Cambridge, United Kingdom, 1965.

34. M. I. Buckett et al., IEEE Transactions on Magnetics MAG-23, No. 2, 1987.

35. M. A. Green, "Development of Large High Current Density Superconducting Solenoid Magnet for use in High Energy Physics Experiments," Dr. of Engineering Thesis, Lawrence Berkeley Laboratory report, LBL-5350, May 1977.

36. A. K. Ghosh and W. B. Sampson, Advances in Cryogenic Engineering 32, Plenum Press, New York, 1986.

37. P. Dubots et al., IEEE Transactions on Magnetics MAG-21, No. 3, 1985.

38. A. Fevier et al., Advances in Cryogenic Engineering 32, p. 747, Plenum Press, New York, 1986.

39. A. K. Ghosh et al., IEEE Transactions on Magnetics MAG-23, No. 2, 1987.

40. A. K. Ghosh et al., "The Effect of Magnetic Impurities and Barriers on the Magnetization of Fine Filament Nb-Ti Composites," to be published in IEEE Transactions on Magnetics MAG-24, No. 2, 1988.

41. M. Taylor, private communication, a graph given to the author in 1972 at a meeting at the Rutherford Laboratory.

42. A. K. Ghosh, Brookhaven National Laboratory, private communication, magnetization data for superconductor with 19.3-and 8.7-μm filaments taken in 1985 (unpublished).

43. A. K. Ghosh, Brookhaven National Laboratory, private communication concerning magnetization data on two fine filamentary superconductors measured by BNL on April 4, 1985 (unpublished).

44. A. K. Ghosh, Brookhaven National Laboratory, private communication concerning magnetization data on large filament SSC superconductor measured by BNL on April 3, 1985 (unpublished).

45. A. K. Ghosh and W. B. Sampson, Brookhaven National Laboratory, private communication concerning magnetization data on 8.4-μm filament diameter SSC superconductor measured by BNL on October 22, 1986 (unpublished).

46. W. H. Warnes and D. C. Larbalestier, Cryogenics 26, p. 643, December 1986.

47. M. S. Lubell, Advances in Cryogenic Engineering 11, p. 653, 1965.

48. A. El Bindari, R. E. Bernet, and L. O. Hoppie, Advances in Cryogenic Engineering 13, 1967.

49. R. C. Wolgast, H. P. Hernandez, P. R. Aron, H. C. Hitchcock, and K. A. Soloman, Advances in Cryogenic Engineering 8, p. 601, 1962.

50. G. Morgan, "Analytic Forms for Critical Current Data," SSC-MD-84, December 1984.

51. M. A. Green, IEEE Transactions on Nuclear Science NS-18, No. 3, p. 664, 1971.

52. M. A. Green, "Field Generated within the SSC Magnets Due to Persistent Currents in the Superconductor," Proceedings of the Workshop on Accelerator Physics for the Superconducting Super Collider, Ann Arbor, MI, Lawrence Berkeley Laboratory report, LBL-17249, December 1983.

53. W. C. Brown et al., IEEE Transactions on Magnetics MAG-21, No. 2, p. 979, 1985.

54. H. E. Fisk and A. D. McInturff, private communication on the use of passive superconductor to correct the residual field higher multipoles.

55. M. A. Green, IEEE Transactions on Magnetics MAG-23, No. 2, p. 506, 1987.

56. A. Asner, IEEE Transactions on Magnetics MAG-23, No. , p. 514, 1987.

57. M. A. Green, "Modeling the Behavior of Oriented Permanent Magnet Material Using Current Doublet Theory", to be published in IEEE Transactions on Magnetics MAG-24, No. 2, 1988.

58. A. K. Ghosh, Brookhaven National Laboratory, private communication on the temperature dependence of the width of magnetization curves.

59. W. B. Sampson et al., IEEE Transactions on Magnetics MAG-15, No. 1, p. 114, 1979.

60. H. M. Ledbetter, Advances in Cryogenic Engineering 24, p. 103, 1978.

61. Handbook on Materials for Superconducting Machinery, Metals and Ceramics Center, Battelle Columbus Ohio Laboratories, MED-HB-04, November 1974.

62. R. P. Reed et al., Advances in Cryogenic Engineering 22, p. 463.

63. J. W. Ekin, IEEE Transactions on Magnetics MAG-23, No. 2, p. 1634, 1987.

64. P. A. Sanger et al., IEEE Transactions on Magnetics MAG-17, No. 1, p. 666, 1981.

65. J. W. Ekin, IEEE Transactions on Magnetics MAG-15, No. 1, p. 197, 1979.

66. W. Specking et al., Advances in Cryogenic Engineering 26, p. 568, Plenum Press, New York, 1980.

67. G. Rupp, Advances in Cryogenic Engineering 26, p. 522, Plenum Press, New York, 1980.

68. J. W. Ekin, IEEE Transactions on Magnetics MAG-17, No. 1, p. 658, 1981.

69. S. Murase et al., IEEE Transactions on Magnetics MAG-21, No. 2, p. 316, 1985.

70. J. W. Ekin, IEEE Transactions on Magnetics MAG-19, No. 3, p. 900, 1983.

71. D. C. Howe et al., IEEE Transactions on Magnetics MAG-19, No. 3, p. 423, 1983.

72. J. Marty and J. C. Vallier, IEEE Transactions on Magnetics MAG-17, No. 5, p. 1635, 1981.

73. D. C. Howe and T. L. Francavilla, Advances in Cryogenic Engineering 26, p. 402, Plenum Press, New York, 1980.

74. K. Tachikawa et al., IEEE Transactions on Magnetics MAG-15, No. 1, p. 391, 1981.

75. D. V. Gubser et al., IEEE Transactions on Magnetics MAG-17, No. 1, p. 1360, 1981.

76. C. L. H. Thieme et al., IEEE Transactions on Magnetics MAG-21, No. 2, p. 756, 1985.

LAWRENCE BERKELEY LABORATORY
TECHNICAL INFORMATION DEPARTMENT
UNIVERSITY OF CALIFORNIA
BERKELEY, CALIFORNIA 94720